

# V-IRL: Grounding Virtual Intelligence in Real Life

Jihan Yang<sup>1\*</sup> Runyu Ding<sup>1</sup> Ellis Brown<sup>2</sup> Xiaojuan Qi<sup>1</sup> Saining Xie<sup>2</sup>  
<sup>1</sup>The University of Hong Kong <sup>2</sup>New York University

<https://virl-platform.github.io>

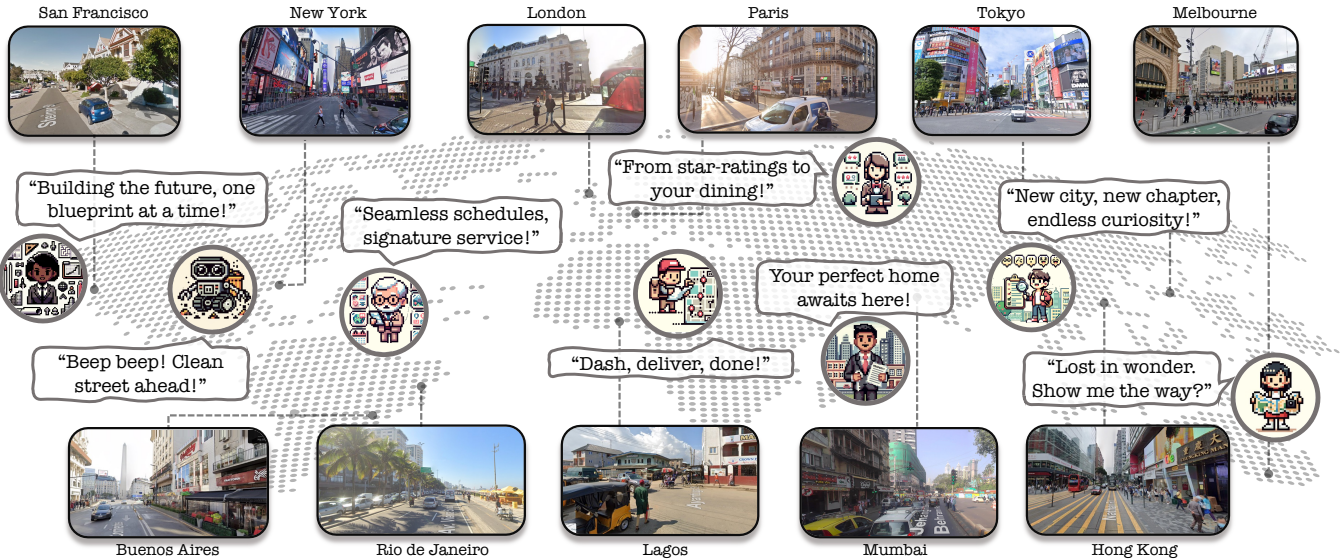


Figure 1. V-IRL agents leverage real-world geospatial information and street view imagery to navigate urban terrains, execute complex tasks, and interact in real-time scenarios. From recommending relevant destinations to assessing city infrastructure to collaboratively giving & following verbal directions—we develop agents that illustrate V-IRL’s current capabilities, flexibility, and utility. Above all else, we present a flexible platform for researchers to harness abundant data from across the globe to create and test diverse autonomous agents.

## Abstract

There is a sensory gulf between the Earth that humans inhabit and the digital realms in which modern AI agents are created. To develop AI agents that can sense, think, and act as flexibly as humans in real-world settings, it is imperative to bridge the realism gap between the digital and physical worlds. How can we embody agents in an environment as rich and diverse as the one we inhabit, without the constraints imposed by real hardware and control? Towards this end, we introduce V-IRL: a platform that enables agents to scalably interact with the real world in a virtual yet realistic environment. Our platform serves as a playground for developing agents that can accomplish various practical tasks and as a vast testbed for measuring progress in capabilities spanning perception, decision-making, and interaction with real-world data across the entire globe.

## 1. Introduction

The advent of large language models (LLMs) has breathed new life into autonomous agent research by offering a universal interface for diverse capabilities, ranging from basic reasoning to complex planning and tool use [78]. While these developments are promising, most of these agents remain confined to text-based environments or simplistic simulations. Visual components in existing agents are either rudimentary—such as simulated tabletop environments [12, 31]—or rely on abstracted representations using ground-truth APIs [30, 73]. Furthermore, the prevalent visual models employed by these agents are trained on photogenic, object-centric Internet images, which fail to capture the unpredictability and diversity of real-world scenes.

This paper aims to bridge this gap between AI agents and the sensory world by grounding them in rich, real-world environments—a crucial step towards developing autonomous agents that can effectively operate in real-life sce-

\*Work conducted during a visit to NYU.

narios. Our novel setting for AI agents *necessitates* rich sensory grounding and perception: virtual embodiment within cities around the globe using real visual and geospatial data.

To this end, we introduce *V-IRL*, a versatile platform for building and testing virtual agents within this novel virtual-real-world setting. *V-IRL* harnesses the power of mapping and street view data, enabling agents to navigate real-world locations, access up-to-date information about their surroundings, and perform practical tasks. With geospatial coordinates at its core, *V-IRL* is flexible and extensible, integrating with arbitrary geospatial platforms and APIs. Moreover, *V-IRL* opens up a vast sea of visual data, allowing a simple and extensible way for researchers to evaluate vision models on realistic data distributions.

We demonstrate the versatility and adaptability of *V-IRL* by developing a series of diverse exemplar agents, each solving a unique and practical task. As these agents hinge upon foundational language and vision models, it is critical to evaluate these models within this setting and their impact on agent performance. We leverage the vast data available through our platform to develop *global scale* benchmarks measuring the performance of underlying vision models on images from diverse geographic and cultural contexts—evaluating their adaptability to shifting environmental, architectural, and language-specific elements. Furthermore, we evaluate the contributions of models to agent performance on challenging tasks. Our results illustrate the potential of *V-IRL* in bridging the gap between virtual agents and visually rich real-world environments, paving the way for future research in this direction.

In summary, our contributions are:

- **V-IRL**: an open-source platform for building and testing agents in a real-world setting that *necessitates* rich sensory grounding and perception—embodiment using real geospatial data and street-view imagery.
- Development of **diverse exemplar agents** that showcase the platform’s versatility and adaptability.
- **Global benchmarks** measuring the performance of foundational language and vision models (1) in isolation using our platform’s real-world data and (2) on end-to-end agent performance in challenging tasks. In addition, we **discuss the robustness of “open-world” vision models to real-world data from across the globe.**

We are excited to see how the research community will leverage *V-IRL* to develop and test agents that can understand and interact with the real world.

## 2. Related Work

Here, we ground *V-IRL* to three streams of research.

**AI Agents.** Agents are autonomous entities capable of perceiving their environment and acting to achieve goals [75]. Historically, agent development has leveraged symbolic and reinforcement learning methods [10, 33, 54], which face is-

ues of scalability and real-world utility. In contrast, the new wave of LLM-driven agents overcomes these challenges with text as a universal interface, enabling natural human interaction and adaptability to various tasks [55, 68, 69, 74, 84]. Moreover, these models equip agents with complex capabilities, such as tool use and collaboration [29, 38, 56, 61, 73, 77, 92]. Yet a critical limitation persists: the agents in this new wave are entirely text-based, devoid of any tangible connection to the visual or sensory aspects of the real world.





**Embodied AI.** Embodied AI studies intelligent agents & robots perceiving and interacting with their environment. A significant challenge in this field is the acquisition of large quantities of realistic data. Consequently, robots are primarily trained in simulated environments [13, 51, 60, 79, 80] to develop skills such as navigation [4, 5, 14] and manipulation [28, 86]. Recent advancements in LLMs [2, 6, 72] have enabled embodied agents to perform long-horizon and open-end tasks in game-engines [30, 31, 43, 50, 66] or human rooms [11, 12, 22, 32, 42]. However, the diversity of tasks and data is still too narrow and simplistic to enable them to operate flexibly in diverse real-world environments.

**Open-World Computer Vision.** Motivated by the success of vision-language models [3, 8, 57, 87] pre-trained on large-scale web-crawled data [18, 35, 62, 67, 71, 81], open-world computer vision has received increasing attention in recent years [21, 26, 36, 37, 40, 52, 82, 83, 90]. However, images and benchmarks sourced from the Internet [7, 20, 24, 34, 36, 59] are unavoidably biased towards specific distributions rather than truly reflecting the real world [58]. Because they are trained and evaluated entirely on Internet data, existing “open-world” models are effectively more open-*Internet* than open-*world*.

## 3. Virtual Intelligence in Real Life

To demonstrate the versatility of *V-IRL*, we use it to instantiate several exemplar agents in our virtual real-world environment. In this section, we engage these agents with tasks that highlight various capabilities of our platform. In Sec. 4, we discuss the technical details of our platform and how it enables agents to interact with the real world.

For illustration, we give *V-IRL* agents character metadata, including an 8-bit avatar, a name, a short bio, and an intention they are trying to accomplish. More concretely, agents are defined by pipelines that use this character metadata along with our platform’s API and pretrained models to address complex tasks (see Sec. 4). Here we provide a high-level overview of the tasks, highlight the *V-IRL* capabilities they require, and visualize the agents solving them.

We highlight the specific *V-IRL* capabilities being employed throughout using tags and corresponding colored underlines:  Map → action,  LLM → reasoning,  Vision → perception, &  Colab → collaboration.

### 3.1. Earthbound Agents

V-IRL agents inhabit virtual representations of real cities around the globe. At the core of this representation are *geographic coordinates* corresponding to points on the Earth’s surface. Using these coordinates, V-IRL allows virtual agents to *ground* themselves in the real world using maps, street view imagery, information about nearby destinations, and additional data from arbitrary geospatial APIs.



Aria searches for possible restaurants nearby. She then synthesizes public reviews to make final recommendations via GPT-4. As Peng is new to the city and originally from Sichuan, she recommends a spicy Chinese joint *Kwa Food Deep Fried Skewers* to give him a taste of home.

*Peng hires Vivek to help him find an apartment in East Village, Jersey City, or Long Island City for \$1k–\$3k per month close to a gym, supermarket, and public transit. . .*

**Route Optimizer** ENV Map

---

**Name:** Peng **Age:** 21 **Loc:** NYC  
**Bio:** Originally from Chengdu, Sichuan, Peng is a student at PKU. He just arrived for a semester abroad at NYC, and is couch surfing until he gets settled.  
**Intention:** Peng needs to visit five locations around the city: his University Card Center, Residence Hall, Research Center, Library, and Student Center.

**Task:** Given a starting address and a list of waypoints, plan the shortest route to all waypoints and then follow it on street view.

**Takeaway:** V-IRL instantiates agents with *real* geospatial information, and enables useful tasks like route optimization.

*Peng needs to visit several locations throughout the city to get documents signed for registration as a visiting student. . .*

Leveraging Geolocation & Mapping capabilities, Peng saves 7 minutes by walking along the shortest path as opposed to in order waypoint visitation as shown in Fig. 2.

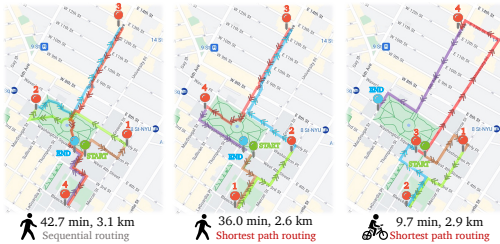


Figure 2. Finding the shortest path for Peng to travel to five places.

### 3.2. Language-Driven Agents

To tackle more complex tasks, we follow the pattern of language-driven agents [78]. LLMs enable agents to flexibly reason, plan, and use external tools & APIs.

**Place Recommender** ENV Map LM LLM

---

**Name:** Aria **Age:** 26 **Loc:** NYC  
**Bio:** A 3rd year graduate student who loves to try new restaurants. She is always looking for new places to try, and shares her favorite spots on her blog!  
**Intention:** Pick out a lunch spot that Peng might like.

**Name:** Vivek **Age:** 35 **Loc:** NYC  
**Bio:** A tech-savvy estate agent who combines his local knowledge with online tools like Zillow to find the perfect homes for his clients in the bustling city.  
**Intention:** Help Peng find a place to live for the semester.

**Task:** Given specific location, background, and intention, synthesize reviews of nearby businesses to provide a recommendation.

**Takeaway:** V-IRL exposes rich real-world information to agents that they can use for real-world tasks.

*Peng is starving for some lunch but doesn’t know where to eat. . . Luckily, he met a nice grad student Aria during his errands who might be able to help him find a good spot. . .*

**Recommendations** Rental Information

---

**Personalized rating: 7.5/10**  
 The apartment is well-located with easy access to supermarkets, public transport, and a gym, which aligns with Peng’s requirements. However, the price may not be cost-effective for a student.

**Personalized rating: 8/10**  
 The apartment is well-located near a supermarket and gym, which aligns with Peng’s lifestyle. Multiple bus stations are nearby, but the lack of a close subway station may affect his commute.

**Personalized rating: 2/10**  
 The estate lacks nearby supermarkets, bus, subway stations, and gyms, which are essential for Peng’s requirements.

Vivek uses real estate APIs to find potential apartments in Peng’s desired regions and price range. For each candidate, he re-searches its proximity to the places Peng cares about. Synthesizing these factors, Vivek provides a holistic rating and accompanying reasoning using GPT-4. His top recommendation is a cost-effective 1 bedroom apartment for \$1986/mo, which is close to a supermarket, 2 bus stations, and a gym.

### 3.3. Visually Grounded Agents

Although language-driven agents can address some real-world tasks using external tools, their reliance solely on text-based information limits their applicability to tasks where *visual grounding* is required. In contrast, *real sensory input* is integral to many daily human activities—allowing a deep connection to and understanding of the world around us. Agents can leverage street view imagery through the V-IRL platform to *visually ground* themselves in the real world—opening up a wide range of *perception-driven tasks*.

**Urban Assistance Robot** ENV Map Vision

---

**Name:** RX-399 **Age:** Unk. **Loc:** HK/NYC  
**Bio:** This urban robot’s advanced object detection, localization, and navigational telemetry systems allow it to perform perceptive tasks in busy city streets.  
**Intention:** Report the locations of trash bins to the sanitation dept.

**Task:** Travel along a specified route and detect instances of a specified object (e.g., trash bins, hydrants, benches, etc.).

**Takeaway:** V-IRL agents can use perceptive input to understand and interact with their environment.

*RX-399 is a state-of-the-art robot agent with advanced navigation and sensing capabilities. Its manufacturer is running a pilot program with sanitation departments in Hong Kong and New York City to assess its readiness for garbage duty. . .*

RX-399 navigates along pre-defined city routes, tagging all trash bins using its open-world detector and geolocation module as depicted in Fig. 4. RX-399 can actively adjust its camera pose to the optimal view for each potential ob-

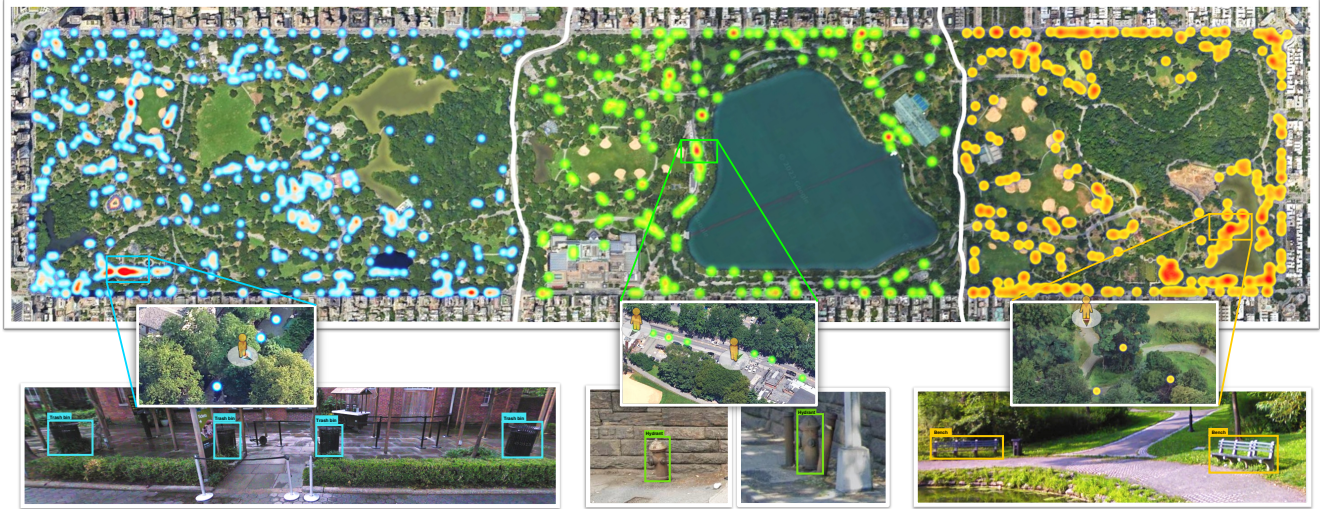


Figure 3. Imani’s visualization of trash bins, fire hydrants, & park benches in NYC’s Central Park using data collected by RX-399.

ject thanks to our interactive embodied environment and the sensor-rich visual input. *During the pilot in Hong Kong, RX-399 locates eight trash bins, correctly identifying five but overlooking one. In New York, it accurately detects all five trash bins but mistakenly reports two mailboxes.*

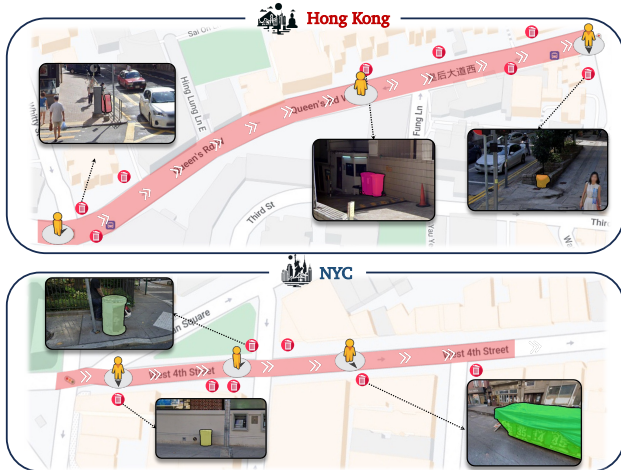


Figure 4. Portions of RX-399’s system records in HK and NYC.

RX-399 can avoid double-counting previously seen objects by using feature matching to check for duplicates among prior detections (see Fig. 5).



Figure 5. RX-399 avoids double-counting trash cans by identifying duplicates across different viewpoints using feature matching.

Urban Planner
ENV Map Vision

**Name:** Imani    **Age:** 42    **Loc:** NYC

**Bio:** A sustainable urban development graduate, Imani is passionate about maintaining a harmonious balance between nature and urban ecosystems.

**Intention:** Use RX-399 to collect first-person data for her studies.

**Task:** Record the location of all instances of any specified objects (e.g., trash bins, hydrants, benches, etc.) in a specified region.

**Takeaway:** V-IRL enables realistic open-world applications requiring vast geospatial and first-person visual information.

*Imani needs to analyze the distribution of trash bins, fire hydrants, and park benches in New York’s Central Park for a project with the NYC Parks & Recreation department. . .*

Imani sets routes spanning Central Park and objects of interest for RX-399, who traverses the routes and records all detected instances. After RX-399 finishes its route, Imani analyzes the collected data at different levels of detail. As depicted in Fig. 3, the coarsest level shows general distributions of trash bins, hydrants, and benches in the park. Imani can also zoom in to specific regions, where lighter colors represent positions with more unique instances identified. The following table presents RX-399’s counting report:

Category	Trash Bin	Fire Hydrant	Park Bench*
Count	1059	727	1015

Table 1. RX-399’s counting report in Central Park, New York City. (\*Note: contiguous benches counted as one instance).

By retrieving geotagged sensory-rich data within RX-399, Imani can also inspect the detection results for each object to help her verify the reliability of RX-399’s reports as illustrated by the bottom level in Fig. 3.

**Intentional Explorer** ENV Map LLM CV Vision


---

**Name:** Hiro **Age:** 22 **Loc:** HK  
**Bio:** A seasoned traveler, Hiro thrives in unknown territories. He enjoys getting lost in new places instead of following the travel guide.  
**Intention:** Hiro is looking for an authentic lunch spot that is not too spicy.

**Task:** Explore on foot (in street view) looking for a destination that fulfills a certain intention (e.g., lunch, shopping, etc.)

**Takeaway:** Agents can utilize visual detectors, VLMs and LLMs to iteratively perceive, decide, and interact in the environment.

*Hiro is starting a new journey in Hong Kong. He decides to explore without a specific destination in mind, looking for a good local lunch spot with food that's not too spicy...*

As depicted in Fig. 6, starting at , Hiro walks down the street and encounters the first intersection. Thanks to the interactive and sensory-rich environment, he can adjust his pose to fetch street views for each possible path. Using VQA on these views, he decides to turn left:

★ *Residential buildings on the left road indicate cozy and family-run local food... A better choice than the others!*

Then, after exploring for a block, he encounters the second intersection where he looks around and decides to turn right:

★ *Looks like there are some local food spots this way...*

After a few steps, Hiro finds “A One Chinese Noodles 阿一豬扒酸辣米線” using his open-world detector. He retrieves information, ratings, and reviews for the restaurant using our platform, which connects street views to places. Hiro ultimately decides to pass on it and keep exploring because:

★ *Most reviews mention the spicy pork chop noodles...*


Finally, at the end of the block , Hiro discovers another lunch spot called “Xintianfa 新天發”. He decides to dine there after reading numerous online reviews praising its authentic cuisine and diverse menu.



Figure 6. Visualization for Hiro’s lunch exploration in HK.

### 3.4. Collaborative Agents

Humans often work together to solve complex real-world tasks. This collaboration promotes efficiency and effectiveness by decomposing a complex task into simpler sub-tasks, allowing each to be handled by an expert in its domain. Grounded in the world via our platform, *V-IRL* agents can leverage geospatial data and street view imagery to collaborate with other agents as well as with human users.

#### 3.4.1 Agent-Agent Collaboration

As with previous agents, collaborative agents are designed for specific tasks; however, they can handle objectives beyond their expertise through collaboration with each other.

**Tourist** ENV Map LLM CV Vision COL Colab

---

**Name:** Ling **Age:** 25 **Loc:** NYC/SF/HK  
**Bio:** Ling is a spirited traveler from Taipei who is always eager to explore new cities and cultures. She is unafraid of asking locals for help when she's lost!  
**Intention:** NYC: find gifts for friends back home, go to a famous restaurant. SF: find a store to repair a broken iPhone. HK: try some authentic local food.

**Task:** (i) Ask a nearby Local agent for directions to a specific location. The Locals will preview the route on the map and in streetview and then provide walking directions in natural language, mentioning major intersections and landmarks.  
(ii) Follow these directions in streetview, and if lost, ask another Local agent for assistance.

**Takeaway:** Agents can collaborate to solve complex tasks that are beyond their individual expertise.

*Ling travels to cities around the world. She seeks out authentic experiences and is always unafraid to ask for help from Locals whenever she finds herself lost...*

After obtaining route descriptions from Locals, Ling starts her journey—as shown in Fig. 7. Grounded in our embodied platform, Ling can adjust her pose and identify visual landmarks along the streets using open-world recognition and her map. Correctly recognizing these landmarks helps GPT-4 to make correct decisions about where to change direction, move forward, and stop, as seen in the top two New York City cases in Fig. 7. The success of these decisions made by GPT-4 relies on the real-sensory input for visual grounding and the interactive environment from *V-IRL*.

Nevertheless, Ling may occasionally fail to find the destination. In the bottom left San Francisco example in Fig. 7, Ling passes by the Apple Store because only its stainless steel wall is visible from her viewpoint. In the bottom right Hong Kong example, Ling mistakes another restaurant for her destination and stops prematurely. Fortunately, when she makes these mistakes, Ling can ask another Local agent for new directions and start another round of navigation, which eventually leads her to the destination.

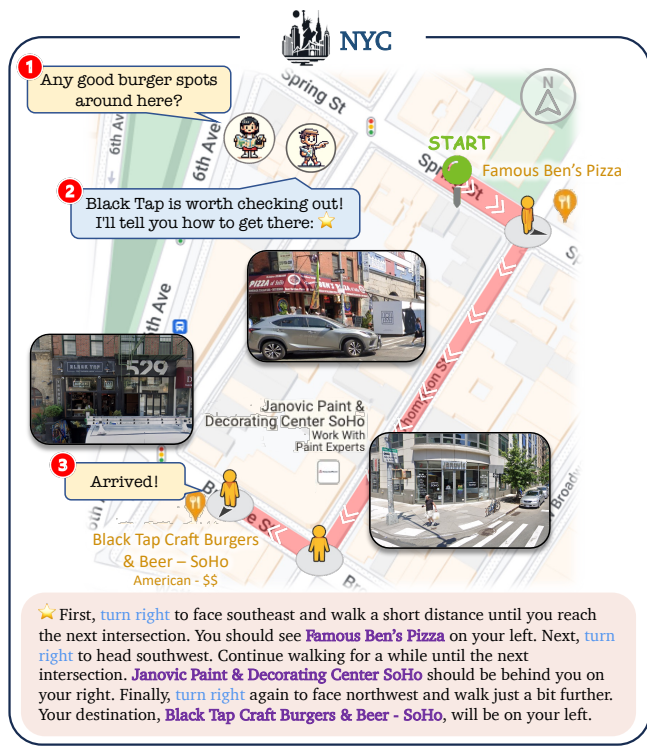
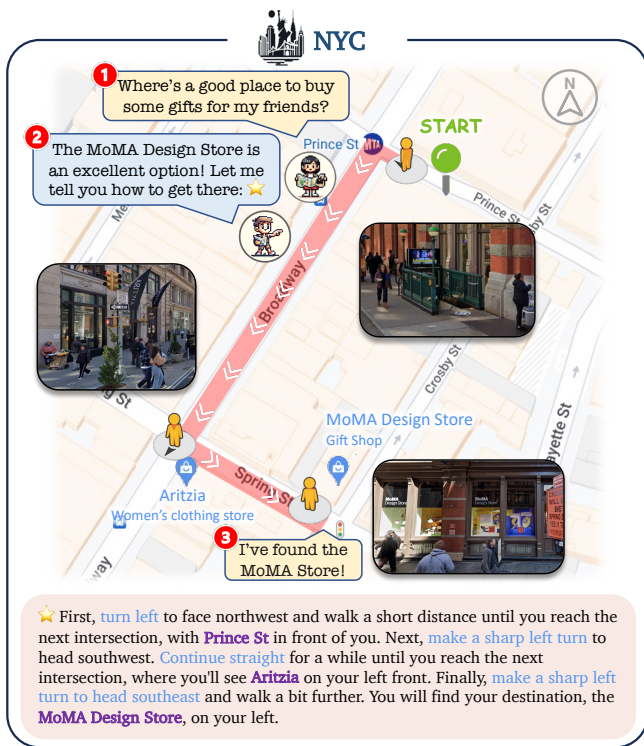


Figure 7. Ling and Local collaboration examples. Trajectories in red and green mean Ling's first and second attempts, respectively.

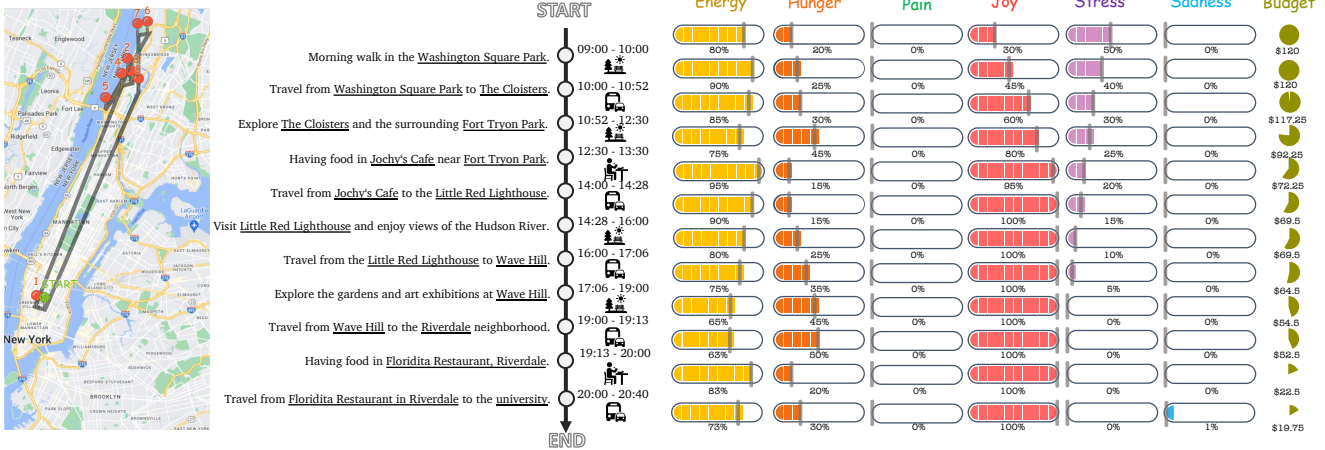


Figure 8. *The Perfect Day Itinerary*: Crafted by Diego, our iterative concierge agent, this schedule is meticulously tailored, accounting for your mental and physical well-being and budget variations as your day unfolds.



Figure 9. Diego traverses regions of interest to find scenic locations to add to your itinerary.

### 3.4.2 Human-Agent Collaboration

Grounded in the same environment we humans inhabit, V-IRL agents can collaborate with and assist real human users.

**Interactive Concierge** ENV Map L LLM CV Vision COL Colab

**Name:** Diego    **Age:** 62    **Loc:** NYC

**Bio:** Diego is an expert concierge at a hotel. He's a master at creating intricate itineraries and providing valuable local advice.

**Intention:** Plan personalized and practical itinerary for customer!

**Task:** Given a user's location, background, and intention for a day, plan a full itinerary balancing their mental/physical state & budget.

**Takeaway:** V-IRL agents can collaborate with users to solve complex tasks that require understanding the user's internal state.

*As a university student in NYC, you are excited to spend a day exploring lesser-known and tranquil places. Your friend recommended Diego, who is known for his professionalism in planning practical and personalized itineraries.*

As depicted in Fig. 8, Diego's itinerary is tailored to *your* (the user's) needs. Diego not only considers your physical and mental interoception status, budget for each activity, but also anticipates your status changes and cost when you follow each event. He is able to take into account *real travel times* from the V-IRL platform and select suitable destinations by collaborating with another recommendation agent.

In contrast, Fig. 10 shows that a simpler "ungrounded" LLM-only concierge agent is unable to consider the real dis-



Figure 10. An ungrounded LLM-only concierge agent's itinerary.

tance and travel time between locations without access to V-IRL, resulting in an impractical itinerary. For example, lacking real geospatial information, the ungrounded concierge allocates only *30 minutes* for travel between the "Brooklyn Botanic Garden" and "Wave Hill" in the Bronx, which actually requires *60–100 minutes\**. The hallucinated travel times overlook geospatial realities and result in a plan with excessively distant destinations.

Also, as shown in Fig. 11, you can intervene in Diego's

\* (per Google Maps <https://maps.app.goo.gl/SW1r5GSx3ZV67BT7r>).

planning process by adjusting your interoceptive status or by providing verbal feedback. In response, Diego promptly revises his original plan to accommodate your demands, and re-estimates your state changes after his revision.

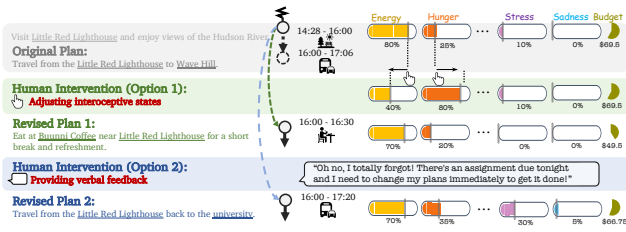


Figure 11. Diego adapts original plan to suit user’s intervention.

Finally, using *V-IRL*’s street views and *Map*, Diego can traverse regions of interest scouting for potential scenic viewpoints for you to visit as shown in Fig. 9. He uses *VQA* to rate and assess each captured view, and adds the highest-rated locations to your itinerary.

## 4. System Fundamentals

This section introduces our system’s core: a platform designed for perception-driven agents that transforms real-world cities around the world into a vast virtual playground where agents can be constructed to solve practical tasks. At its heart, *V-IRL* is comprised of a hierarchical architecture (see Fig. 12). The *platform* lies at the foundation—providing the underlying components and infrastructure for agents to employ. Higher level *capabilities* of *CV* Perception, *LM* Reasoning, *ENV* Action, and *COL* Collaboration emerge from the platform’s components. Finally, *agents* leverage these capabilities and user-defined metadata in task-specific routines to solve tasks.

### 4.1. Agent Definition

In our system, agent behavior is shaped by user-defined metadata, including a background, an intended goal, and an interoceptive state. The *background* provides the context necessary to instantiate the agent in the real world (location), and to guide its reasoning and decision-making (biography). *Intentions* outline agents’ purpose within the environment. An agent’s *interoceptive state* reflects its internal mental and physical status—varying over time and influencing its behavior. This novel concept is crucial to AI agents for enhancing collaboration with humans (see Sec. 3.4.2).

Concretely, agents are developed by writing task-specific `run()` routines that leverage the various components of our platform and the agent’s metadata to solve tasks.

### 4.2. Platform Components

Next, we delve into the platform components, which provide the infrastructure to instantiate capabilities, execute agent actions, and ground agents in the real world.

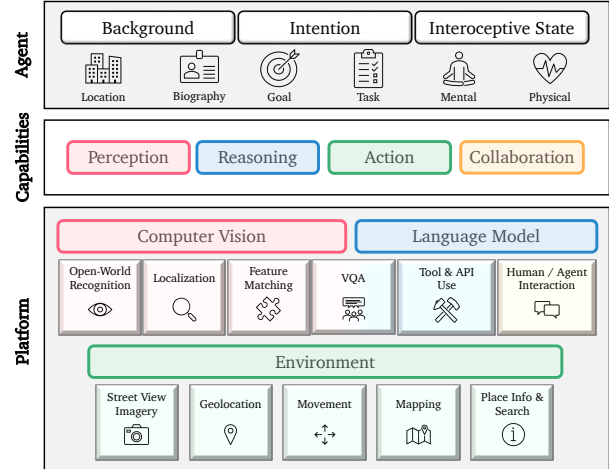


Figure 12. Hierarchical *V-IRL* architecture described in Sec. 4.

#### 4.2.1 Environment (Action)

*ENV* Environment components are responsible for grounding agents in the world around them: providing a navigable representation of real cities (see Sec. 3.1). Geographic coordinates serve as the link between the world and our virtual representation of it. Leveraging the Google Maps Platform (GMP) [27], *V-IRL* enables agents to access street view imagery, query valid movements, retrieve information about nearby locations, and plan routes. As these coordinates and location information are bound to the real world, they also provide a natural interface with external tools that leverage geolocation—such as real estate APIs (see Sec. 3.2). Technical designs of environment are detailed in Appendix C.

#### 4.2.2 Vision (Perception)

*CV* Perception components enable agents to process the sensory-rich data provided by the *environment*, especially street view imagery. Pretrained localization models [40] give agents a precise spatial understanding of their environment. This allows RX-399 to identify and count instances of objects, and Hiro to pick out specific businesses to look up with the *GMP* (Sec. 3.3). While localization models allow for precise interaction with perceptive input, open-world recognition models [57] are more general, and allow agents to detect a wider range of objects in their field of view (e.g., Tourist searches for the Apple Store). Pretrained feature matching models [44] provide an understanding of continuity across views of the same location, and enable agents to identify & deduplicate instances of the same object from different viewpoints (Sec. 3.3). Multimodal models with *VQA* & Captioning capabilities [39] bridge the perceptual world with natural language, and are essential for integration with *reasoning* (Sec. 3.3).



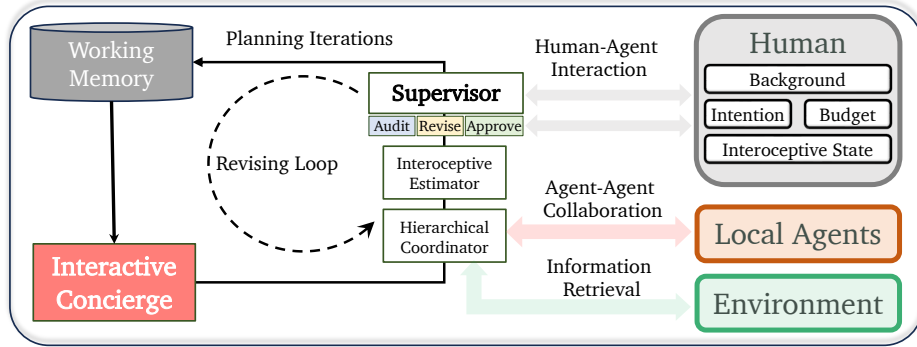


Figure 13. Architecture overview of interactive concierge agent Diego (Sec. 3.4.2). See pipeline description in Sec. 4.4.

### 4.2.3 Language (Reasoning & Collaboration)

**LM Reasoning** components allow decision making based on information from perception and the environment. LLMs such as GPT-4 [2] and Llama 2 [72] interface across various APIs (Sec. 3.2), transforming environmental data and perceptual outputs into actionable insights. They also enable **COL Collaboration** between agents or with humans through natural language (Sec. 3.4) Custom prompts facilitate this interaction (see Sec. 4.4).

### 4.3. V-IRL Capabilities

Our platform’s components can be flexibly combined to exhibit a vast array of capabilities. In Sec. 3, we present agents that exhibit increasingly complex behaviors, each requiring more components of the platform. From simple combinations, like the Route Optimizer (Sec. 3.1), to more complex arrangements, like the Tourist (Sec. 3.4.1), our system showcases the versatility and potential of the V-IRL platform to be applied to various real-world scenarios. Next, we perform a high-level case study of how V-IRL’s components are combined to create our most complex agent; in Appendix D, we delve deeper into the low-level platform details that underpin creating a V-IRL agent.

### 4.4. High-Level System Case Study: Interactive Concierge “Diego”

By studying Diego (Sec. 3.4.2), we illustrate how our platform’s components are combined to create complex agents.

Behind Diego’s proficiency in developing itineraries is his iterative planning pipeline (depicted in Fig. 13). The process begins with Diego creating an initial draft plan for the first activity using GPT-4, taking into account the user’s biography, requirements, and previous activities in working memory. This draft is then meticulously refined. First, a hierarchical coordination module retrieves real transportation time and asks a recommendation agent for dining recommendations. Subsequently, an interoceptive estimation module evaluates the effect of the proposed activity on the user’s mental/physical state and budget.

The crucial final step involves a supervisor module, which reviews (“audits”) the incoming activity in light of the current user status, remaining budget, and potential interactions (exemplified in Fig. 11). If the supervisor deems the plan unsuitable, it initiates revisions. The revised plan is then looped back to the hierarchical coordinator and interoceptive estimator for reliability, followed by another review from the supervisor (see the revising loop in Fig. 13). This iterative process between the hierarchical coordinator, the interoceptive estimator, and the supervisor continues until the supervisor approves the activity and adds it to its working memory.

After finalizing an activity, Diego proceeds to plan the subsequent activity by repeating this process until the day’s itinerary is complete.

## 5. V-IRL Benchmarks

In the previous sections, we illustrate the primary benefit of the V-IRL platform: seamless access to first-person street-view imagery and descriptive information about real-world cities across the globe. This *scalable* source of *truly open-world* data can be harnessed to test core component models and agent capabilities. We propose three V-IRL benchmarks: two evaluating vision-language models on open-world vision tasks (Secs. 5.2 and 5.3), and one evaluating end-to-end agent performance (Sec. 5.4). Benchmark details are in Appendix E.

### 5.1. Automated Data and Annotation Collection

To allow our V-IRL benchmarks to scale globally, we develop an automatic data/annotation construction pipeline instead of crawling and manually annotating limited data. This allows models to be conveniently tested worldwide, provided there is access to Google Street Views [27].

**Region Selection.** Though our benchmark is feasible across all regions covered by the GMP, we select 14 districts across 12 cities from 6 continents to ensure coverage of a diverse

data distribution while keeping inference costs affordable. The detailed locations of these regions are listed in Tab. 2.

**Place Types.** We collect place information in each region for all 96 place types annotated by GMP<sup>†</sup>. Our V-IRL place: detection, recognition and VQA benchmarks are built upon all or part of these place types.

**Vision and Place Data Collection.** Within each region, we collect geolocations with available street views, place information, and place-centric images.

**Data Cleaning.** Though scalable, automated data collection can introduce noise due to the absence of human supervision. To this end, we design three automatic data cleaning strategies: *i)* *distance-based filtering* to exclude places not easily visible from any street views due to their distance; *ii)* *human-review filtering* to remove “zombie” places with no reviews which might no longer be valid or relevant; and *iii)* *CLIP-based filtering* to retain only *place-centric images* with a high CLIP likelihood of being *storefronts*.

**Human Verification.** To validate the quality, we randomly sample over 10% of data from each benchmark. We find that only about 7% of the samples contain errors, which confirms the high quality of our data, particularly given the real-world sources.

Continent	City	District
Africa	Johannesburg	Rosebank
	Lagos	Surulere
Asia	Mumbai	Khar
	New Delhi	Lajpat Nagar
	Hong Kong	Prince Edward
	Tokyo	Shinjuku
Australia	Melbourne	CBD
	Melbourne	SouthBank
Europe	Milan	Brera
	London	Oxford St
North America	New York City	Chinatown, Manhattan
	New York City	SoHo, Manhattan
	San Francisco	Union Square
South America	Buenos Aires	Monserrat

Table 2. Region list for global V-IRL benchmarks.

## 5.2. V-IRL Place: Detection

Every day, humans traverse cities, moving between varied places to fulfill a range of goals, like the Intentional Explorer agent (Sec. 3.3). We assess the performance of vision models on the everyday human activity of *localizing places* using street view imagery and associated place data.

**Setups.** We modify RX-399 (Sec. 3.3) to traverse polygonal areas while localizing & identifying 20 types of places. We subsample 28 polygonal areas from the 14 districts.

<sup>†</sup>[https://developers.google.com/maps/documentation/places/web-service/supported\\_types/#table1](https://developers.google.com/maps/documentation/places/web-service/supported_types/#table1)

**Benchmarked Models.** We evaluate three prominent open-world detection models: GroundingDINO [48], GLIP [40] and Owl-ViT [52], OpenSeeD [89] and Owl-ViT v2 [53]. We also implement a straightforward baseline, CLIP (w/ GLIP proposal), which involves reclassifying the categories of GLIP proposals with CLIP [57].

**Evaluation.** We evaluate the models based on localization recall, which is quantified as  $\frac{N_{tp}}{N_{tp}+N_{fn}}$ , where  $N_{tp}$  and  $N_{fn}$  represents the number of correctly localized places and missed places, respectively.

**Matching between Object Proposals and Places.** As mentioned in Sec. 5.1, we do not annotate bounding boxes for places on each potential street view image. Such human annotation diverges from our initial motivation of providing plug-and-play and sensor-rich (V-IRL) benchmarks. To assign ground truth for each object proposal in this scenario, we develop a simple matching strategy to assign object proposals from street view object detections to nearby places.

As illustrated in Fig. 14, we first project the bounding box of each object proposal onto a frustum in the 3D space, subject to a radius. We then determine if any nearby places fall within this frustum and radius. If any nearby place is found, the closest one is assigned as the *ground truth* for the object proposal. Otherwise, the object proposal is regarded as a *false positive*. When multiple places are inside the frustum, we consider the nearest one as the ground truth since it would likely block the others in the image. *This process is also used in Intentional Explorer agent Hiro to parse object proposals on image to place information.*



Figure 14. Matching between 2D object proposal and street place.

**Results.** Tab. 3 shows that open-world detectors like GroundingDINO [48], Owl-ViT [52] and GLIP [40] are biased towards certain place types such as *school*, *cafe*, and *convenience store*, respectively. In contrast, CLIP (w/ GLIP proposal) can identify a broader spectrum of place types. This is mainly caused by the category bias in object detection datasets with a limited vocabulary. Hence, even if detectors like Owl-ViT are initialized with CLIP, their vocabulary space narrows down due to fine-tuning. These results suggest that cascading category-agnostic object proposals to zero-shot recognizers appears promising for “real” open-world detection—especially for less com-

mon categories in object detection datasets.

Place Types											AR <sup>10</sup>	AR <sup>20</sup>
GroundingDINO [48]	0.0	0.0	0.0	0.0	0.0	4.9	0.0	0.0	100.0	0.0	11.7	5.8
Owl-ViT [52]	0.0	61.0	0.0	0.0	0.0	2.4	0.3	0.0	0.0	0.0	7.1	7.1
GLIP [40]	20.0	0.0	100.0	0.0	0.0	0.0	18.4	0.0	0.0	0.0	15.4	9.0
OpenSeeD [89]	60.0	11.9	50.0	0.0	0.0	0.0	20.5	0.0	0.0	16.7	17.7	16.7
Owl-ViT v2 [53]	0.0	0.0	0.0	0.0	0.0	0.0	0.0	0.0	0.0	0.0	0.0	3.4
CLIP [57] (w/ GLIP proposal)	60.0	6.8	50.0	40.0	25.0	29.3	14.7	0.0	0.0	16.7	26.9	23.7

Table 3. Benchmark results on *V-IRL Place Detection*. AR<sup>10</sup> and AR<sup>20</sup> denote average recall on subsampled 10 and all 20 place categories, respectively. Full results in Appendix E.1.

### 5.3. *V-IRL Place*: Recognition and VQA

In contrast to the challenging *V-IRL place detection* task using street view imagery alone, in real life, humans can recognize businesses by taking a closer, place-centric look. We assess existing vision models in this manner on two perception tasks based on place-centric images: *i*) recognizing specific place types; *ii*) identifying human intentions via Vision Question Answering (VQA).

**Setups.** For recognition, we assess 10 open-world recognition models on identifying a place’s type (from 96 options) using place-centric images (see Tab. 4). For place VQA, we evaluate 13 multi-modal large language models (MM-LLM) to determine viable human intentions from a four-option multiple-choice. The *V-IRL Place VQA* process is illustrated in Fig. 15, where the candidate and true choices are generated by GPT-4 [2] given the place types and place names corresponding to the image.



**Question:** Which human intentions can be accomplished here?  
**Choices:** A. Learning how to cook authentic Australian food.  
 B. Applying for a reduction on parking fines.  
 C. Reporting a crime or lost property.  
 D. Attending a yoga session.

Figure 15. Example of *V-IRL Place VQA* process.

**Place-centric Images vs. Street View Images.** In contrast to the street view imagery utilized in the *V-IRL Place detection* benchmark, the *V-IRL Place recognition* and VQA benchmarks use place-centric images. To illustrate the distinction between these image types, we present examples in Fig. 16. The figure shows that street view images, sourced from the Google Street View database<sup>‡</sup>, are taken from the



Figure 16. Top row: examples of street view imagery. Bottom row: corresponding place-centric images.

street and encompass a broader view of the surroundings, including multiple buildings and possible occluding objects/vehicles. In contrast, place-centric images, drawn from the Google Place database<sup>§</sup>, are taken on foot and focus more closely on the specific place—providing a more concentrated view.

**Evaluation.** We adopt mean accuracy (mAcc) to evaluate both place recognition and VQA tasks. For place VQA, we follow MMBench [49] to conduct circular evaluation and GPT-assisted answer parsing.

	Model	#Param	mAcc (%)
<b><i>V-IRL Place Recognition</i></b>			
CLIP [57]	ViT-B/32	151M	18.2
CLIP [57]	ViT-L/14	428M	37.2
CLIP [57]	ViT-L/14@336px	428M	41.3
OpenCLIP [18]	ViT-B/32	151M	21.2
OpenCLIP [18]	ViT-L/14	428M	31.0
Eva-02-CLIP [70]	ViT-B/16	150M	19.5
Eva-02-CLIP [70]	ViT-L/14	428M	34.2
Eva-02-CLIP [70]	ViT-L/14@336px	428M	40.7
SigLIP [88]	ViT-B/16	203M	29.5
SigLIP [88]	ViT-L/16@384px	652M	37.3
<b><i>V-IRL Place VQA</i></b>			
MiniGPT-4 [91]	Vicuna-13B-v0	14B	3.9
mPLUG-Owl [85]	LLaMA-7B	7B	5.5
Shikra [16]	Vicuna-7B	7B	10.9
BLIP-2 [39]	FlanT5 <sub>XXL</sub>	12B	69.6
InstructBLIP [19]	FlanT5 <sub>XXL</sub>	12B	68.0
LLaVA [46]	Vicuna-13B-v1.3	13B	23.5
LLaVA-1.5 [45]	Vicuna-7B-v1.5	7B	60.1
LLaVA-1.5 [45]	Vicuna-13B-v1.5	13B	61.9
LLaVA-NeXT [47]	Vicuna-7B-v1.5	7B	65.9
Mini-Gemini [41]	Vicuna-7B-v1.5	7B	44.1
Intern-VL-1.5 [17]	InternLM2-20B	26B	77.6
GPT-4V [2]	UNK.	UNK.	77.1
Qwen-VL-max [9]	UNK.	UNK.	74.3

Table 4. Benchmark results on *V-IRL Place recognition* and *V-IRL Place VQA*. Green indicates increased resolution models, while Blue denotes model parameter scaling.

streetview

<sup>§</sup><https://developers.google.com/maps/documentation/places/web-service/photos>

<sup>‡</sup><https://developers.google.com/maps/documentation/streetview/request->

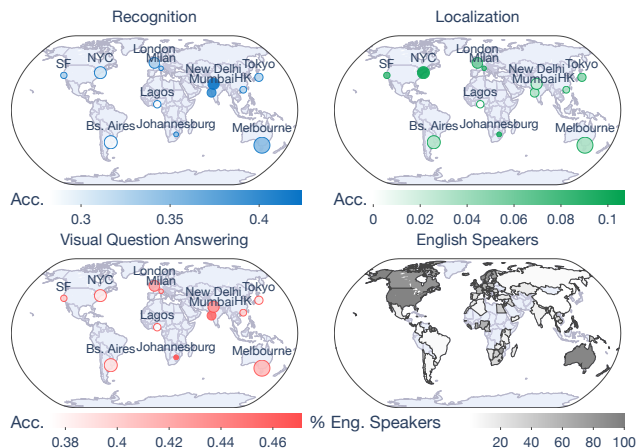


Figure 17. City-level visualization of *V-IRL* benchmark results.

**Results.** Tab. 4 shows that CLIP (L/14@336px) outperforms even the biggest version of Eva-02-CLIP and SigLIP in the *V-IRL* recognition task, highlighting the high-quality data used to train CLIP [57]. The bottom of the table shows that LLaVA-NeXT (7B) outperforms its predecessors LLaVA-1.5 and 1.0, but still has over 8% gap to InternVL-1.5 with 26B parameters. Closed-source MLLMs GPT-4V and Qwen-VL-Max yield outstanding performance compared to most open-sourced models. We note that even these top-performing MLLMs (e.g. GPT-4V and Qwen-VL-Max) still suffer from inconsistent issues during the circular evaluation (see Tab. 7). Moreover, vision models perform better on place VQA over place-type recognition, suggesting direct prompts about human intention could be more effective for intention-driven tasks. We provide more analysis in Appendix E.2.

#### 5.4. *V-IRL* Vision-Language Navigation

As discussed in Sec. 3.3, Intentional Explorer and Tourist agents require coordination between vision models and language models to accomplish vision-language tasks. To investigate the effect of various models on end-to-end agent performance, we develop an embodied task that jointly tests vision and language models: Vision-Language Navigation (VLN). In VLN, agents navigate to a desired destination by following textual directions using only raw street views.

**Setup.** We adopt the Tourist implementation from Sec. 3.4 and swap its recognition component with the various benchmarked models. These models are used to identify visual landmarks during navigation. Subsequently, GPT-4 [2] predicts the next action according to the recognition results. Navigation instructions are generated using the Local agent. Recent work VELMA [65] attempts to enhance VLN by leveraging LLMs on existing datasets [15, 64]. In contrast, our *V-IRL* VLN benchmark evaluates vision models and their coordination with language models across a global data scale. See more details in Appendix E.3.

Method	Start		Intersection		Stop	
	Success	Reac	Arr	Reac	Arr	Reac
Oracle (No Vision)	1.0	1.0	1.0	1.0	1.0	1.0
CLIP (B/32) [57]	0.22	1.0	0.86	0.84	0.83	0.22
CLIP (L/14@336px) [57]	0.44	0.83	0.73	0.94	0.67	0.44
EVA-02-CLIP (BigE/14-plus) [70]	0.39	0.89	0.77	0.94	0.72	0.39
EVA-02-CLIP (L/14@336px) [70]	0.22	1.0	0.82	0.83	0.78	0.22
LLaVA-1.5-13B [45]	0.11	0.61	0.55	1.0	0.56	0.11
PP-OCR [23] (+ GPT3.5)	0.28	0.89	0.73	0.94	0.72	0.28

Table 5. Results on *V-IRL* VLN-mini. We test various CLIP-based models, MM LLM, and OCR model with GPT postprocessing.

**Benchmarked methods.** Four approaches are evaluated to recognize landmarks during navigation: (i) Oracle that searches nearby landmarks with GMP [27]; (ii) Zero-shot recognizers CLIP [57] & EVA-CLIP [70]; (iii) Multi-modal LLM LLaVA-1.5 [45]; (iv) An OCR model [23] to extract text in street views followed by GPT answer parsing. Implementation details are provided in Appendix E.3.

**Evaluation.** We primarily measure navigation success rate (*Success*), defining success as the navigator stopping within 25 meters of the destination. In addition, as navigation success is mainly influenced by the agent’s actions at key positions (i.e., start positions, intersections and stop positions), we also evaluate the arrival ratio (*Arr*) and reaction accuracy (*Reac*) for each route. *Arr* denotes the percentage of key positions reached, while *Reac* measures the accuracy of the agent’s action predictions at these key positions. To save GPT-4 resources, we mainly compare vision modules on a 10% mini-set comprising 18 routes from 9 regions. See Appendix E.3 for full-set results with CLIP and Oracle.

**Results.** Table 5 shows that, with oracle landmark information, powerful LLMs can impressively comprehend navigation instructions and thus make accurate decisions. However, when relying on vision models to fetch landmark information from street views, the success rate drops dramatically—suggesting that the perception of vision models is noisy and misguides LLMs’ decision-making. Among these recognizers, larger variants of CLIP [57] and EVA-02-CLIP [70] perform better, highlighting the benefits of model scaling. LLaVA-1.5 [45] shows inferior performance with CLIP (L/14@336px) as its vision encoder, possibly due to the alignment tax [2] introduced during instruction tuning. Further, PP-OCR [23] (+ GPT-3.5) achieves a 28% success rate, signifying that OCR is crucial for visual landmark recognition.

#### 5.5. Geographic Diversity

Spanning 12 cities across the globe, our *V-IRL* benchmarks provide an opportunity to analyze the inherent model biases across different regions. As depicted in Fig. 17, vision models demonstrate subpar performance on all three benchmark tasks in Lagos, Tokyo, Hong Kong, and Buenos

Aires. Vision models might struggle in Lagos due to its non-traditional street views relative to more developed cities (see street views in Fig. 1). For cities like Tokyo, Hong Kong, and Buenos Aires, an intriguing observation is their primary use of non-English languages in street views, as shown in Fig. 17 bottom right<sup>¶</sup> and Fig. 1. This suggests that existing vision models may face challenges when deployed in non-English-dominant countries.

## 6. Discussion: Ethics & Privacy

Our platform serves as a tool for AI development and as a crucible for ethical discourse and preparation. As AI is inevitably being integrated into society—*e.g.*, via augmented reality wearables, spatial computing platforms, or mobile robots navigating city streets—it is imperative to confront and discuss ethical and privacy concerns now. Unlike these impending *real-time* systems, the data accessed by *V-IRL* is “stale” and preprocessed—providing a controlled environment to study these concerns.

Notably, *V-IRL* exclusively utilizes preexisting, readily available APIs; it does not capture or make available any previously inaccessible data. Our primary source of street-view imagery, Google Maps [27], is subject to major privacy-protection measures, including blurring faces and license plates [25]. Moreover, *V-IRL* complies with the Google Maps Platform license<sup>¶</sup>, similarly to notable existing works that also leverage Google’s street views [1, 15].

We believe *V-IRL* is an invaluable tool for researching bias. As discussed in Sec. 5.5, *V-IRL*’s *global scale* provides a lens to study linguistic, cultural, and other geographic biases inherent in models. By using *V-IRL* to study such questions, we aim to preemptively tackle the ethical dilemmas that will arise with deploying real-time systems rather than being blindsided by them. We hope our work helps spur proactive discussion of future challenges throughout the community.

## 7. Conclusion

In this work, we introduce *V-IRL*, an open-source platform designed to bridge the sensory gap between the digital and physical worlds, enabling AI agents to interact with the real world in a virtual yet realistic environment. Through *V-IRL*, agents can develop rich sensory grounding and perception, utilizing real geospatial data and street-view imagery. We demonstrate the platform’s versatility by creating diverse exemplar agents and developing benchmarks measuring the performance of foundational language and vision models on open-world visual data from across the globe.

This platform opens new avenues for advancing AI capabilities in perception, decision-making, and real-world data

interaction. As spatial computing and robotic systems become increasingly prevalent, the demand for and possibilities of AI agents will only grow. From personal assistants to practical applications like urban planning to life-changing tools for the visually impaired, we hope *V-IRL* helps usher in a new era of perceptually grounded agents.

---

<sup>¶</sup>Source: [https://en.wikipedia.org/wiki/List\\_of\\_countries\\_by\\_English-speaking\\_population](https://en.wikipedia.org/wiki/List_of_countries_by_English-speaking_population)

<sup>¶</sup><https://cloud.google.com/maps-platform/terms>

## References

- [1] Image geo-localization based on multiplenearest neighbor feature matching using generalized graphs. *TPAMI*, 2014. [13](#)
- [2] Josh Achiam, Steven Adler, Sandhini Agarwal, Lama Ahmad, Ilge Akkaya, Florencia Leoni Aleman, Diogo Almeida, Janko Altmenschmidt, Sam Altman, Shyamal Anadkat, et al. GPT-4 technical report. *arXiv preprint arXiv:2303.08774*, 2023. [2](#), [9](#), [11](#), [12](#), [19](#), [24](#)
- [3] Jean-Baptiste Alayrac, Jeff Donahue, Pauline Luc, Antoine Miech, Iain Barr, Yana Hasson, Karel Lenc, Arthur Mensch, Katherine Millican, Malcolm Reynolds, et al. Flamingo: a visual language model for few-shot learning. In *NeurIPS*, 2022. [2](#)
- [4] Peter Anderson, Angel Chang, Devendra Singh Chaplot, Alexey Dosovitskiy, Saurabh Gupta, Vladlen Koltun, Jana Kosecka, Jitendra Malik, Roozbeh Mottaghi, Manolis Savva, et al. On evaluation of embodied navigation agents. *arXiv preprint arXiv:1807.06757*, 2018. [2](#)
- [5] Peter Anderson, Qi Wu, Damien Teney, Jake Bruce, Mark Johnson, Niko Sünderhauf, Ian Reid, Stephen Gould, and Anton Van Den Hengel. Vision-and-Language Navigation: Interpreting visually-grounded navigation instructions in real environments. In *CVPR*, 2018. [2](#)
- [6] Rohan Anil, Andrew M Dai, Orhan Firat, Melvin Johnson, Dmitry Lepikhin, Alexandre Passos, Siamak Shakeri, Emanuel Taropa, Paige Bailey, Zhifeng Chen, et al. PaLM 2 technical report. *arXiv preprint arXiv:2305.10403*, 2023. [2](#)
- [7] Yuki M Asano, Christian Rupprecht, Andrew Zisserman, and Andrea Vedaldi. PASS: An imagenet replacement for self-supervised pretraining without humans. In *NeurIPS*, 2021. [2](#)
- [8] Anas Awadalla, Irena Gao, Josh Gardner, Jack Hessel, Yusuf Hanafy, Wanrong Zhu, Kalyani Marathe, Yonatan Bitton, Samir Gadre, Shiori Sagawa, et al. OpenFlamingo: An open-source framework for training large autoregressive vision-language models. *arXiv preprint arXiv:2308.01390*, 2023. [2](#)
- [9] Jinze Bai, Shuai Bai, Shusheng Yang, Shijie Wang, Sinan Tan, Peng Wang, Junyang Lin, Chang Zhou, and Jingren Zhou. Qwen-vl: A frontier large vision-language model with versatile abilities. *arXiv preprint arXiv:2308.12966*, 2023. [11](#), [24](#)
- [10] Christopher Berner, Greg Brockman, Brooke Chan, Vicki Cheung, Przemysław Dębniak, Christy Dennison, David Farhi, Quirin Fischer, Shariq Hashme, Chris Hesse, et al. Dota 2 with large scale deep reinforcement learning. *arXiv preprint arXiv:1912.06680*, 2019. [2](#)
- [11] Anthony Brohan, Noah Brown, Justice Carbajal, Yevgen Chebotar, Xi Chen, Krzysztof Choromanski, Tianli Ding, Danny Driess, Avinava Dubey, Chelsea Finn, Pete Florence, Chuyuan Fu, Montse Gonzalez Arenas, Keerthana Gopalakrishnan, Kehang Han, Karol Hausman, Alex Herzog, Jasmine Hsu, Brian Ichter, Alex Irpan, Nikhil Joshi, Ryan Julian, Dmitry Kalashnikov, Yuheng Kuang, Isabel Leal, Lisa Lee, Tsang-Wei Edward Lee, Sergey Levine, Yao Lu, Henryk Michalewski, Igor Mordatch, Karl Pertsch, Kanishka Rao, Krista Reymann, Michael Ryoo, Grecia Salazar, Pannag Sanketi, Pierre Sermanet, Jaspier Singh, Anikait Singh, Radu Soricut, Huong Tran, Vincent Vanhoucke, Quan Vuong, Ayzan Wahid, Stefan Welker, Paul Wohlhart, Jialin Wu, Fei Xia, Ted Xiao, Peng Xu, Sichun Xu, Tianhe Yu, and Brianna Zitkovich. RT-2: Vision-language-action models transfer web knowledge to robotic control. *arXiv preprint arXiv:2307.15818*, 2023. [2](#)
- [12] Anthony Brohan, Yevgen Chebotar, Chelsea Finn, Karol Hausman, Alexander Herzog, Daniel Ho, Julian Ibarz, Alex Irpan, Eric Jang, Ryan Julian, et al. Do As I Can, Not As I Say: Grounding language in robotic affordances. In *CoRL*, 2023. [1](#), [2](#)
- [13] Angel Chang, Angela Dai, Thomas Funkhouser, Maciej Halber, Matthias Niessner, Manolis Savva, Shuran Song, Andy Zeng, and Yinda Zhang. Matterport3D: Learning from rgb-d data in indoor environments. In *3DV*, 2017. [2](#)
- [14] Devendra Singh Chaplot, Dhiraj Prakashchand Gandhi, Abhinav Gupta, and Russ R Salakhutdinov. Object goal navigation using goal-oriented semantic exploration. In *NeurIPS*, 2020. [2](#)
- [15] Howard Chen, Alane Suhr, Dipendra Misra, Noah Snaveley, and Yoav Artzi. TOUCHDOWN: Natural language navigation and spatial reasoning in visual street environments. In *CVPR*, 2019. [12](#), [13](#)
- [16] Keqin Chen, Zhao Zhang, Weili Zeng, Richong Zhang, Feng Zhu, and Rui Zhao. Shikra: Unleashing multimodal llm’s referential dialogue magic. *arXiv preprint arXiv:2306.15195*, 2023. [11](#)
- [17] Zhe Chen, Weiyun Wang, Hao Tian, Shenglong Ye, Zhangwei Gao, Erfei Cui, Wenwen Tong, Kongzhi Hu, Jiapeng Luo, Zheng Ma, et al. How far are we to gpt-4v? closing the gap to commercial multimodal models with open-source suites. *arXiv preprint arXiv:2404.16821*, 2024. [11](#), [24](#)
- [18] Mehdi Cherti, Romain Beaumont, Ross Wightman, Mitchell Wortsman, Gabriel Ilharco, Cade Gordon, Christoph Schuhmann, Ludwig Schmidt, and Jenia Jitsev. Reproducible scaling laws for contrastive language-image learning. In *CVPR*, 2023. [2](#), [11](#)
- [19] Wenliang Dai, Junnan Li, Dongxu Li, Anthony Meng Huat Tiong, Junqi Zhao, Weisheng Wang, Boyang Li, Pascale Fung, and Steven Hoi. InstructBLIP: Towards General-purpose Vision-Language Models with Instruction Tuning. In *NeurIPS*, 2023. [11](#), [21](#)
- [20] Jia Deng, Wei Dong, Richard Socher, Li-Jia Li, Kai Li, and Li Fei-Fei. ImageNet: A large-scale hierarchical image database. In *CVPR*, 2009. [2](#)
- [21] Runyu Ding, Jihan Yang, Chuhui Xue, Wenqing Zhang, Song Bai, and Xiaojuan Qi. Pla: Language-driven open-vocabulary 3d scene understanding. In *Proceedings of the IEEE/CVF conference on computer vision and pattern recognition*, pages 7010–7019, 2023. [2](#)
- [22] Danny Driess, Fei Xia, Mehdi S. M. Sajjadi, Corey Lynch, Aakanksha Chowdhery, Brian Ichter, Ayzan Wahid, Jonathan Tompson, Quan Vuong, Tianhe Yu, Wenlong Huang, Yevgen Chebotar, Pierre Sermanet, Daniel Duckworth, Sergey Levine, Vincent Vanhoucke, Karol Hausman, Marc Toussaint, Klaus Greff, Andy Zeng, Igor Mordatch, and Pete Florence. PaLM-E: An Embodied Multimodal Language Model. In *ICML*, 2023. [2](#)

- [23] Y Du, C Li, R Guo, X Yin, W Liu, J Zhou, Y Bai, Z Yu, Y Yang, Q Dang, et al. PP-OCR: A practical ultra lightweight ocr system. *arXiv preprint arXiv:2009.09941*, 2020. 12, 24
- [24] Abhimanyu Dubey, Vignesh Ramanathan, Alex Pentland, and Dhruv Mahajan. Adaptive methods for real-world domain generalization. In *CVPR*, 2021. 2
- [25] Andrea Frome, German Cheung, Ahmad Abdulkader, Marco Zennaro, Bo Wu, Alessandro Bissacco, Hartwig Adam, Hartmut Neven, and Luc Vincent. Large-scale privacy protection in google street view. In *ICCV*, 2009. 13
- [26] Golnaz Ghiasi, Xiuye Gu, Yin Cui, and Tsung-Yi Lin. Scaling open-vocabulary image segmentation with image-level labels. In *ECCV*, 2022. 2
- [27] Google Map Team. Google Map Platform. <https://mapsplatform.google.com/>. 8, 9, 12, 13
- [28] Shixiang Gu, Ethan Holly, Timothy Lillicrap, and Sergey Levine. Deep reinforcement learning for robotic manipulation with asynchronous off-policy updates. In *ICRA*, 2017. 2
- [29] Sirui Hong, Mingchen Zhuge, Jonathan Chen, Xiawu Zheng, Yuheng Cheng, Ceyao Zhang, Jinlin Wang, Zili Wang, Steven Ka Shing Yau, Zijuan Lin, Liyang Zhou, Chenyu Ran, Lingfeng Xiao, Chenglin Wu, and Jürgen Schmidhuber. MetaGPT: Meta Programming for A Multi-Agent Collaborative Framework. In *ICLR*, 2023. 2
- [30] Wenlong Huang, Pieter Abbeel, Deepak Pathak, and Igor Mordatch. Language Models As Zero-Shot Planners: Extracting actionable knowledge for embodied agents. In *ICML*, 2022. 1, 2
- [31] Wenlong Huang, Fei Xia, Ted Xiao, Harris Chan, Jacky Liang, Pete Florence, Andy Zeng, Jonathan Tompson, Igor Mordatch, Yevgen Chebotar, et al. Inner Monologue: Embodied reasoning through planning with language models. In *CoRL*, 2022. 1, 2
- [32] Wenlong Huang, Chen Wang, Ruohan Zhang, Yunzhu Li, Jiajun Wu, and Li Fei-Fei. VoxPoser: Composable 3d value maps for robotic manipulation with language models. *arXiv preprint arXiv:2307.05973*, 2023. 2
- [33] Heinrich Küttler, Nantas Nardelli, Alexander Miller, Roberta Raileanu, Marco Selvatici, Edward Grefenstette, and Tim Rocktäschel. The nethack learning environment. In *NeurIPS*, 2020. 2
- [34] Alina Kuznetsova, Hassan Rom, Neil Alldrin, Jasper Uijlings, Ivan Krasin, Jordi Pont-Tuset, Shahab Kamali, Stefan Popov, Matteo Mallocci, Alexander Kolesnikov, et al. The Open Images Dataset V4: Unified image classification, object detection, and visual relationship detection at scale. *IJCV*, 2020. 2
- [35] Hugo Laurençon, Lucile Saulnier, Léo Tronchon, Stas Bekman, Amanpreet Singh, Anton Lozhkov, Thomas Wang, Siddharth Karamcheti, Alexander M Rush, Douwe Kiela, et al. OBELICS: An open web-scale filtered dataset of interleaved image-text documents. In *NeurIPS*, 2023. 2
- [36] Alexander C Li, Ellis Brown, Alexei A Efros, and Deepak Pathak. Internet explorer: Targeted representation learning on the open web. In *International Conference on Machine Learning*, pages 19385–19406. PMLR, 2023. 2
- [37] Boyi Li, Kilian Q Weinberger, Serge Belongie, Vladlen Koltun, and Rene Ranftl. Language-driven semantic segmentation. In *ICLR*, 2022. 2
- [38] Guohao Li, Hasan Abed Al Kader Hammoud, Hani Itani, Dmitrii Khizbullin, and Bernard Ghanem. CAMEL: Communicative agents for "mind" exploration of large language model society. In *NeurIPS*, 2023. 2
- [39] Junnan Li, Dongxu Li, Silvio Savarese, and Steven Hoi. BLIP-2: bootstrapping language-image pre-training with frozen image encoders and large language models. In *ICML*, 2023. 8, 11
- [40] Liunian Harold Li, Pengchuan Zhang, Haotian Zhang, Jianwei Yang, Chunyuan Li, Yiwu Zhong, Lijuan Wang, Lu Yuan, Lei Zhang, Jenq-Neng Hwang, et al. Grounded language-image pre-training. In *CVPR*, 2022. 2, 8, 10, 11
- [41] Yanwei Li, Yuechen Zhang, Chengyao Wang, Zhisheng Zhong, Yixin Chen, Ruihang Chu, Shaoteng Liu, and Jiaya Jia. Mini-gemini: Mining the potential of multi-modality vision language models. *arXiv preprint arXiv:2403.18814*, 2024. 11
- [42] Jacky Liang, Wenlong Huang, Fei Xia, Peng Xu, Karol Hausman, Brian Ichter, Pete Florence, and Andy Zeng. Code as Policies: Language model programs for embodied control. In *ICRA*, 2023. 2
- [43] Kevin Lin, Christopher Agia, Toki Migimatsu, Marco Pavone, and Jeannette Bohg. Text2Motion: From natural language instructions to feasible plans. *arXiv preprint arXiv:2303.12153*, 2023. 2
- [44] Philipp Lindenberger, Paul-Edouard Sarlin, and Marc Pollefeys. LightGlue: Local Feature Matching at Light Speed. In *ICCV*, 2023. 8
- [45] Haotian Liu, Chunyuan Li, Yuheng Li, and Yong Jae Lee. Improved baselines with visual instruction tuning. *arXiv:2310.03744*, 2023. 11, 12, 24
- [46] Haotian Liu, Chunyuan Li, Qingyang Wu, and Yong Jae Lee. Visual instruction tuning. In *NeurIPS*, 2023. 11, 21
- [47] Haotian Liu, Chunyuan Li, Yuheng Li, Bo Li, Yuanhan Zhang, Sheng Shen, and Yong Jae Lee. Llava-next: Improved reasoning, ocr, and world knowledge, 2024. 11
- [48] Shilong Liu, Zhaoyang Zeng, Tianhe Ren, Feng Li, Hao Zhang, Jie Yang, Chunyuan Li, Jianwei Yang, Hang Su, Jun Zhu, et al. Grounding DINO: Marrying dino with grounded pre-training for open-set object detection. *arXiv preprint arXiv:2303.05499*, 2023. 10, 11
- [49] Yuan Liu, Haodong Duan, Yuanhan Zhang, Bo Li, Songyang Zhang, Wangbo Zhao, Yike Yuan, Jiaqi Wang, Conghui He, Ziwei Liu, et al. MMBench: Is Your Multi-modal Model an All-around Player? *arXiv preprint arXiv:2307.06281*, 2023. 11
- [50] Zeyi Liu, Arpit Bahety, and Shuran Song. REFLECT: Summarizing robot experiences for failure explanation and correction. In *CoRL*, 2023. 2
- [51] Viktor Makoviychuk, Lukasz Wawrzyniak, Yunrong Guo, Michelle Lu, Kier Storey, Miles Macklin, David Hoeller, Nikita Rudin, Arthur Allshire, Ankur Handa, et al. Isaac Gym: High performance gpu-based physics simulation for robot learning. In *NeurIPS*, 2021. 2

- [52] Matthias Minderer, Alexey Gritsenko, Austin Stone, Maxim Neumann, Dirk Weissenborn, Alexey Dosovitskiy, Aravindh Mahendran, Anurag Arnab, Mostafa Dehghani, Zhuoran Shen, et al. Simple Open-Vocabulary Object Detection with Vision Transformers. In *ECCV*, 2022. 2, 10, 11
- [53] Matthias Minderer, Alexey Gritsenko, and Neil Houlsby. Scaling open-vocabulary object detection. *Advances in Neural Information Processing Systems*, 36, 2024. 10, 11
- [54] Volodymyr Mnih, Koray Kavukcuoglu, David Silver, Alex Graves, Ioannis Antonoglou, Daan Wierstra, and Martin Riedmiller. Playing atari with deep reinforcement learning. *arXiv preprint arXiv:1312.5602*, 2013. 2
- [55] Reiichiro Nakano, Jacob Hilton, Suchir Balaji, Jeff Wu, Long Ouyang, Christina Kim, Christopher Hesse, Shantanu Jain, Vineet Kosaraju, William Saunders, et al. WebGPT: Browser-assisted question-answering with human feedback. *arXiv preprint arXiv:2112.09332*, 2021. 2
- [56] Joon Sung Park, Joseph O’Brien, Carrie Jun Cai, Meredith Ringel Morris, Percy Liang, and Michael S Bernstein. Generative Agents: Interactive simulacra of human behavior. In *UIST*, 2023. 2
- [57] Alec Radford, Jong Wook Kim, Chris Hallacy, Aditya Ramesh, Gabriel Goh, Sandhini Agarwal, Girish Sastry, Amanda Askell, Pamela Mishkin, Jack Clark, et al. Learning transferable visual models from natural language supervision. In *ICML*, 2021. 2, 8, 10, 11, 12
- [58] Vikram V Ramaswamy, Sing Yu Lin, Dora Zhao, Aaron Bryan Adcock, Laurens van der Maaten, Deepti Ghadiyaram, and Olga Russakovsky. GeoDE: a geographically diverse evaluation dataset for object recognition. In *NeurIPS*, 2023. 2
- [59] William A Gaviria Rojas, Sudnya Diamos, Keertan Ranjan Kini, David Kanter, Vijay Janapa Reddi, and Cody Coleman. The Dollar Street Dataset: Images representing the geographic and socioeconomic diversity of the world. In *NeurIPS*, 2022. 2
- [60] Manolis Savva, Abhishek Kadian, Oleksandr Maksymets, Yili Zhao, Erik Wijmans, Bhavana Jain, Julian Straub, Jia Liu, Vladlen Koltun, Jitendra Malik, et al. Habitat: A platform for embodied ai research. In *ICCV*, 2019. 2
- [61] Timo Schick, Jane Dwivedi-Yu, Roberto Dessì, Roberta Raileanu, Maria Lomeli, Luke Zettlemoyer, Nicola Cancedda, and Thomas Scialom. Toolformer: Language models can teach themselves to use tools. In *NeurIPS*, 2023. 2
- [62] Christoph Schuhmann, Romain Beaumont, Richard Vencu, Cade W Gordon, Ross Wightman, Mehdi Cherti, Theo Coombes, Aarush Katta, Clayton Mullis, Mitchell Wortsman, Patrick Schramowski, Srivatsa R Kundurthy, Katherine Crowson, Ludwig Schmidt, Robert Kaczmarczyk, and Jenia Jitsev. LAION-5b: An open large-scale dataset for training next generation image-text models. In *NeurIPS*, 2022. 2
- [63] John Schulman, Barret Zoph, Christina Kim, Jacob Hilton, Jacob Menick, Jiayi Weng, Juan Felipe Ceron Uribe, Liam Fedus, Luke Metz, Michael Pokorny, et al. ChatGPT: Optimizing language models for dialogue. *OpenAI blog*, 2022. 24
- [64] Raphael Schumann and Stefan Riezler. Generating landmark navigation instructions from maps as a graph-to-text problem. In *ACL*, 2020. 12, 19
- [65] Raphael Schumann, Wanrong Zhu, Weixi Feng, Tsu-Jui Fu, Stefan Riezler, and William Yang Wang. VELMA: Verbalization embodiment of llm agents for vision and language navigation in street view. *arXiv preprint arXiv:2307.06082*, 2023. 12, 19, 24
- [66] Hao Shao, Yuxuan Hu, Letian Wang, Steven L Waslander, Yu Liu, and Hongsheng Li. LMDrive: Closed-loop end-to-end driving with large language models. *arXiv preprint arXiv:2312.07488*, 2023. 2
- [67] Piyush Sharma, Nan Ding, Sebastian Goodman, and Radu Soricut. Conceptual Captions: A cleaned, hypernymed, image alt-text dataset for automatic image captioning. In *ACL*, 2018. 2
- [68] Noah Shinn, Beck Labash, and Ashwin Gopinath. Reflexion: an autonomous agent with dynamic memory and self-reflection. In *NeurIPS*, 2023. 2
- [69] Significant Gravitass. AutoGPT. <https://github.com/Significant-Gravitas/AutoGPT>, 2023. 2
- [70] Quan Sun, Yuxin Fang, Ledell Wu, Xinlong Wang, and Yue Cao. EVA-CLIP: Improved Training Techniques for CLIP at Scale. *arXiv preprint arXiv:2303.15389*, 2023. 11, 12
- [71] Bart Thomee, David A Shamma, Gerald Friedland, Benjamin Elizalde, Karl Ni, Douglas Poland, Damian Borth, and Li-Jia Li. YFCC100M: The new data in multimedia research. *Communications of the ACM*, 2016. 2
- [72] Hugo Touvron, Louis Martin, Kevin Stone, Peter Albert, Amjad Almahairi, Yasmine Babaei, Nikolay Bashlykov, Soumya Batra, Prajjwal Bhargava, Shruti Bhosale, et al. LLAMA 2: Open foundation and fine-tuned chat models. *arXiv preprint arXiv:2307.09288*, 2023. 2, 9
- [73] Guanzhi Wang, Yuqi Xie, Yunfan Jiang, Ajay Mandlekar, Chaowei Xiao, Yuke Zhu, Linxi Fan, and Anima Anandkumar. Voyager: An open-ended embodied agent with large language models. *arXiv preprint arXiv:2305.16291*, 2023. 1, 2
- [74] Jason Wei, Xuezhi Wang, Dale Schuurmans, Maarten Bosma, Fei Xia, Ed Chi, Quoc V Le, Denny Zhou, et al. Chain-of-thought prompting elicits reasoning in large language models. In *NeurIPS*, 2022. 2
- [75] Michael Wooldridge and Nicholas R Jennings. Intelligent Agents: Theory and practice. *The knowledge engineering review*, 1995. 2
- [76] Penghao Wu and Saining Xie. V\*: Guided Visual Search as a Core Mechanism in Multimodal LLMs. *arXiv preprint arXiv:2312.14135*, 2023. 18
- [77] Qingyun Wu, Gagan Bansal, Jieyu Zhang, Yiran Wu, Shaokun Zhang, Erkang Zhu, Beibin Li, Li Jiang, Xiaoyun Zhang, and Chi Wang. AutoGen: Enabling next-gen llm applications via multi-agent conversation framework. *arXiv preprint arXiv:2308.08155*, 2023. 2
- [78] Zhiheng Xi, Wenxiang Chen, Xin Guo, Wei He, Yiwen Ding, Boyang Hong, Ming Zhang, Junzhe Wang, Senjie Jin, Enyu Zhou, et al. The rise and potential of large language model based agents: A survey. *arXiv preprint arXiv:2309.07864*, 2023. 1, 3
- [79] Fei Xia, Amir R Zamir, Zhiyang He, Alexander Sax, Jitendra Malik, and Silvio Savarese. Gibson Env: Real-world perception for embodied agents. In *CVPR*, 2018. 2



- [80] Fanbo Xiang, Yuzhe Qin, Kaichun Mo, Yikuan Xia, Hao Zhu, Fangchen Liu, Minghua Liu, Hanxiao Jiang, Yifu Yuan, He Wang, et al. SAPIEN: A simulated part-based interactive environment. In *CVPR*, 2020. 2
- [81] Hu Xu, Saining Xie, Xiaoqing Ellen Tan, Po-Yao Huang, Russell Howes, Vasu Sharma, Shang-Wen Li, Gargi Ghosh, Luke Zettlemoyer, and Christoph Feichtenhofer. Demystifying clip data. *arXiv preprint arXiv:2309.16671*, 2023. 2
- [82] Jiarui Xu, Shalini De Mello, Sifei Liu, Wonmin Byeon, Thomas Breuel, Jan Kautz, and Xiaolong Wang. GroupViT: Semantic segmentation emerges from text supervision. In *CVPR*, 2022. 2
- [83] Jihan Yang, Runyu Ding, Weipeng Deng, Zhe Wang, and Xiaojuan Qi. Regionplc: Regional point-language contrastive learning for open-world 3d scene understanding. In *Proceedings of the IEEE/CVF Conference on Computer Vision and Pattern Recognition*, pages 19823–19832, 2024. 2
- [84] Shunyu Yao, Jeffrey Zhao, Dian Yu, Nan Du, Izhak Shafran, Karthik Narasimhan, and Yuan Cao. ReAct: Synergizing reasoning and acting in language models. In *ICLR*, 2023. 2
- [85] Qinghao Ye, Haiyang Xu, Guohai Xu, Jiabo Ye, Ming Yan, Yiyang Zhou, Junyang Wang, Anwen Hu, Pengcheng Shi, Yaya Shi, et al. mPLUG-Owl: Modularization empowers large language models with multimodality. *arXiv preprint arXiv:2304.14178*, 2023. 11
- [86] Sriram Yenamandra, Arun Ramachandran, Karmesh Yadav, Austin Wang, Mukul Khanna, Theophile Gervet, Tsung-Yen Yang, Vidhi Jain, Alexander William Clegg, John Turner, et al. HomeRobot: Open-vocabulary mobile manipulation. In *CoRL*, 2023. 2
- [87] Lu Yuan, Dongdong Chen, Yi-Ling Chen, Noel Codella, Xiyang Dai, Jianfeng Gao, Houdong Hu, Xuedong Huang, Boxin Li, Chunyuan Li, et al. Florence: A new foundation model for computer vision. *arXiv preprint arXiv:2111.11432*, 2021. 2
- [88] Xiaohua Zhai, Basil Mustafa, Alexander Kolesnikov, and Lucas Beyer. Sigmoid loss for language image pre-training. *arXiv preprint arXiv:2303.15343*, 2023. 11
- [89] Hao Zhang, Feng Li, Xueyan Zou, Shilong Liu, Chunyuan Li, Jianwei Yang, and Lei Zhang. A simple framework for open-vocabulary segmentation and detection. In *Proceedings of the IEEE/CVF International Conference on Computer Vision*, pages 1020–1031, 2023. 10, 11
- [90] Xingyi Zhou, Rohit Girdhar, Armand Joulin, Philipp Krähenbühl, and Ishan Misra. Detecting twenty-thousand classes using image-level supervision. In *ECCV*, 2022. 2
- [91] Deyao Zhu, Jun Chen, Xiaoqian Shen, Xiang Li, and Mohamed Elhoseiny. MiniGPT-4: Enhancing Vision-Language Understanding with Advanced Large Language Models. *arXiv preprint arXiv:2304.10592*, 2023. 11
- [92] Xizhou Zhu, Yuntao Chen, Hao Tian, Chenxin Tao, Weijie Su, Chenyu Yang, Gao Huang, Bin Li, Lewei Lu, Xiaogang Wang, Yu Qiao, Zhaoxiang Zhang, and Jifeng Dai. Ghost in the Minecraft: Generally capable agents for open-world environments via large language models with text-based knowledge and memory. *arXiv preprint arXiv:2305.17144*, 2023. 2

## A. Appendix Outline

In these supplementary materials, we provide additional details for our *V-IRL* platform, including:

- Designs behind *V-IRL* Agents (Appendix B);
- Technical details and challenges in the *V-IRL* environment (Appendix C).
- A low-level case study of Intentional Explorer agent Hiro, delving into implementation details of our system such as LLM prompts (Appendix D);
- More detailed setups and results for our *V-IRL* benchmarks (Appendix E).

## B. Technical Details of *V-IRL* Agents

In Sec. 3, our discussion mainly focuses on the innovative capabilities and behaviors of *V-IRL* agents empowered by our platform. We avoid in-depth discussions about technical details in the main paper due to the concern of readability. In this section, we go through our main technical designs for each agent. More comprehensive technical implementations are available in our released code.

### B.1. Peng: Route Optimizer

Peng is designed to showcase the utilization of real geographic coordinates within our platform. By processing a sequence of real addresses, Peng calculates the shortest path for traversing them using various modes of transportation, such as walking, driving, and bicycling, among others. This capability is powered by the mapping module described in Appendix C.3. After that, Peng proceeds to navigate through the destinations along the predetermined path, employing the point navigation procedure outlined in Appendix C.2.2.

### B.2. Aria: Place Recommender

Aria leverages the realistic place information provided by our Place Info & Search module (see Appendix C.4) to enhance LLMs’ reasoning capability in the geographic aspect. Specifically, Aria evaluates Peng’s intention to determine the suitable type of place and searches all possible places in the vicinity. For each searched place, Aria considers its reviews and user ratings from Google to summarize a place overview. Subsequently, we customize prompts for Aria to amalgamate Peng’s biography, intentions, and the summarized place overviews to rate each place between 0 and 10, accompanied by justifications.

Without such technical designs, LLMs could recommend some places that are either too distant or permanently closed. This issue arises because LLMs struggle to accurately understand geospatial relationships and often depend on outdated databases.

### B.3. Vivek: Estate Agent

The process employed by Vivek is similar to that of Aria, as both are designed to recommend places. However, Vivek showcases the versatility of our *V-IRL* platform by demonstrating how it can seamlessly integrate a wide range of realistic information beyond the Google Maps Platform, with a standardized definition of geographic coordinates. This capability enables the creation of even more sophisticated and intriguing agents.

### B.4. RX-399: Urban Assistance Robot

Different from previous example agents, RX-399 introduces visual perception capabilities such as open-world detection and feature matching. There are two fundamental systems inside it – navigation and perception. In terms of navigation, RX-399 can automatically navigate from the current position to the pre-defined destination step by step. This navigation process is elaborated in Appendix C.2.2, and thus, will not be extensively discussed here.

When it comes to its perception system, RX-399 is designed to simulate human visual perception by capturing street views within a 90-degree horizontal angle to both its left and right. For each captured view, an open-world detection process is conducted. Leveraging the interactive capabilities of our environment, we further propose an active detection strategy to dynamically adjust the agent’s ego-pose and focal length according to the scale and position of potential objects. This significantly improves its performance as illustrated in Tab. 6. In the future, more advanced approaches such as visual search [76] could also be considered. In the subsequent de-duplication procedure, which aims to avoid double-counting objects across different viewpoints, we have tried a few strategies including measuring with multi-view geometry, object tracking, and feature matching. We choose feature matching because of its accuracy and efficiency.

City	Hong Kong	New York City
w/ active detection	<b>0.63 / 0.83</b>	<b>0.71 / 1.00</b>
w/o active detection	0.10 / 0.33	0.30 / 0.60

Table 6. RX-399 detection performance with or without active detection manner. Metrics are accuracy / recall.

### B.5. Imani: Urban Planner

The visual perception system of Imani mirrors that of RX-399. The primary distinction between them lies in their navigation systems. Imani possesses the capability to plan a navigation route in the given polygonal region, enabling RX-399 to traverse that region. This functionality is named “region navigation” and elaborated in Appendix C.2.2. Additionally, within the Imani agent, we develop a heatmap visualization tool to visualize and verify the data collected by RX-399 (see Fig. 3).

## B.6. Hiro: Intentional Explorer

Hiro is a representative agent equipped with geographical, perceptual, and reasoning abilities, to address a daily human task: randomly exploring to find a suitable restaurant. In this regard, we have dedicated a separate section to offer an in-depth case study, including the detailed methodology and prompts in Appendix D.

## B.7. Ling: Tourist

Our vision language navigation pipeline of Ling is similar to [65], leveraging vision models, the map, and LLMs. At each position, we start by capturing eight street views around the agent, corresponding to *front*, *left front*, *left*, *left behind*, *behind*, *right behind*, *right* and *right front*. Vision models use these street views to identify landmarks mentioned in route descriptions, which are then verbalized as *landmark observations*. Also, intersection information is retrieved from the mover to formulate an *intersection observation*. LLMs play a crucial role in processing landmark & intersection observations along with the agent’s previous working history to determine the next action. After each action, current observations and actions are stored into the agent’s working history. This auto-regressive process continues until the agent decides to `stop`.

## B.8. Local Agent

The primary mission of the Local agent is to generate human-like and easily followable navigation instructions on a global scale (refer to 3.4.1). This task is known as navigation instruction generation [64]. Contrary to most existing research, which depends on human-annotated data for limited geographic areas, our “Local” agent automatically selects suitable landmarks taking account into real-world places and generates human-like route descriptions using LLMs across the globe. Remarkably, it achieves this without the need for any training data, relying solely on our tailored prompts and a few in-context examples. The effectiveness of its generated instructions has been verified through collaboration with “Ling”. To the best of our knowledge, this is a first in the field. There are massive technical details on selecting easily noticeable landmarks and prompt engineering, which are available in our released code.

## B.9. Diego: Interactive Concierge

In Sec. 4.4, we have already presented the technical designs of Diego’s itinerary. Here, we detail how Diego can find scenic locations as shown in Fig. 9. For any given destination, such as “Fort Tryon Park”, Diego will sample a rectangle region around it and traverse all navigable positions within it. At each position, he will capture a photograph (*i.e.* street view imagery) using pre-defined headings, pitches, and FOVs. Each photograph will then be evaluated

using GPT-4(V) [2], where it receives a rating between 0 and 10 along with explanatory reasons.

## C. Technical Details of Environment

In Sec. 4.2.1, we provide an overview of our system’s environment, which grounds agents in real life. Here, we delve into the technical designs beyond mere leveraging Google Map Platform system calls. Concrete implementations can be found in our open-sourced code.

### C.1. Geolocation & Street View Imagery

At the core of V-IRL lies its innovative use of sensor-rich environment, including street view imagery and geolocations. They enable agents to gather surrounding place and vision information.

**Geolocation.** Agents in the V-IRL platform inhabit virtual representations of real cities around the globe. At the core of this representation are geographic coordinates (*i.e.* geolocation) corresponding to points on the Earth’s surface. The initial geolocation of each agent is specified by its “Location” configuration, as illustrated in Fig. 12. Whenever agents require access to surrounding information (*e.g.* street views, places or maps), geolocation serves as a crucial parameter for querying the related Google Map APIs.

**Street view imagery.** Google Map Platform specifies each street view imagery with multiple key parameters: geolocation, heading (the horizontal angle ranging from  $0^\circ$  to  $360^\circ$ ), pitch (a vertical angle ranging from  $-90^\circ$  to  $90^\circ$ ), and Field of View (FOV, ranging from  $20 \sim 120$ ). It’s noteworthy that adjusting the FOV here is similar to changing the camera’s focal length, rather than simply zooming in on an image, which ensures that image resolution remains high, even as the FOV decreases to a low value. By modifying the heading, pitch, and FOV, we can simulate the human sensory process of adjusting one’s pose and concentrating on a specific area.

#### Alignment between street view imagery and geolocation.

Within our sensor-rich platform, a fundamental challenge is to ensure agents are positioned at geolocations where street view imagery is available. To address this issue, we design a custom operation named “*relocate*”. Specifically, when an agent is initialized at a location lacking street view imagery, the “relocate” operation will identify and transition the agent to the nearest viable geolocation where street view data is available. Notice that, this operation is indispensable to our platform, as the positions with available street views are relatively sparse in comparison to the vast continuous space of all possible coordinates.

### C.2. Movement

Enabling agents to move along city streets is a core functionality of our platform, allowing interaction between

agents and the real world. Whenever an agent needs to move, this module powers all related processes, from route planning and direction selection to the continuous update of the agent’s geolocation during its moving. Since Google Maps Platform does not provide APIs to access nearby navigable positions and directions, the design of this movement module is a significant technical challenge and a substantial contribution from our team. We discuss its low-level implementations in Appendix C.2.1 and the enabled high-level actions in Appendix C.2.2.

### C.2.1 Mover

**Move by controlling the web interface.** A straightforward solution is to let the agent control the web front-end Google Street View to select moving directions and move. Nevertheless, there are three key challenges for this solution:

(i) *How can Python-implemented agents control the movement via the interaction to the webpage?* We use a Python package Selenium\*\* to locate web elements responsible for movement. After determining a movement direction, the agent uses Selenium to simulate a click action on the web element corresponding to the chosen direction.

(ii) *How can the agent acquire the necessary information to decide moving direction?* Although agents can access all potential movement directions from web elements, they cannot identify these directions without prior knowledge of what each represents. We find that the “transform” attribute in the web element corresponding to each direction can be leveraged to calculate their represented heading angles. The heading angle also allows us to collect street view imagery for each movement direction. Agent’s movement decision-making is then based on these heading angles and the visual data from street view imagery.

(iii) *How to track the agent’s geolocation along its movement?* To accomplish this, we customize a webpage element to display the geolocation of the current street view panorama. As the agents move and trigger updates to the street view panorama, this customized element concurrently refreshes to reflect the new geolocation. By using Selenium, we can then extract this updated geolocation data, enabling continuous tracking of the agent’s geolocation changes.

**Move by grid-based relocating.** In our test of the above web-based mover, a critical limitation emerged: the web-embedded Google Street View panoramas display only a subset of navigable directions. This constraint significantly restricts our agents’ mobility, often preventing them from successfully navigating to their intended destinations due to the incomplete coverage of potential routes.

To overcome this obstacle, we develop an alternative method: a grid-based relocating mover. This approach involves performing a grid search for geolocations in the

vicinity of the agent and employing the “relocate” operation to sift through these locations, identifying those that are navigable. While this method offers a more comprehensive view of navigable positions, it is markedly more time-consuming than the web-based approach due to the extensive number of Google Maps API calls required.

In our practical applications, we design a heuristic strategy that combines web-based controlling and grid-based relocation. This hybrid approach aims to balance the trade-offs between the speed and the completeness of navigable position data, optimizing our agents’ capabilities and efficiency in real-world scenarios.

### C.2.2 Navigator

Here, we introduce the high-level action of agents powered by the mover – navigation. Unlike the mover, which concentrates on enabling agent mobility in the environment, the focus here shifts to determining the direction of movement. In our platform, we group different navigators according to their usages into four types:

(i) **Point navigator** is designed to tackle navigation tasks that clearly define single or multiple destinations (represented in addresses or geolocations). This navigator employs the route planning function described in Appendix C.3 to obtain a series of key positions for navigation. At each location, the agent utilizes a greedy algorithm to select the most optimal direction towards the next key position that has not yet been reached. Exemplary agents, such as “Peng”, “RX-399” and “Local”, use this type of navigator in their implementation.

(ii) **Region navigator** is tailored for agents like “Imani” and “Diego”, who need to traverse every position within a polygonal region. This navigator first employs a grid search combined with our “relocate” operation to identify all navigable positions within the specified region. Subsequently, it adopts a heuristic algorithm designed to solve the traveling salesman problem, planning an efficient order for visiting these positions. The agents’ task is to simply follow this predetermined route, visiting each navigable position in the planned order.

(iii) **Vision-language navigator** is specifically developed for the tourist agent “Ling”, as well as for tasks within the V-IRL vision-language navigation benchmark. Its primary function is to guide the agent in selecting a proper direction based on navigation instructions. The detailed pipeline is presented in Appendix B.7.

(iv) **Intention navigator** is utilized in intentional explorer agent “Hiro” to select the most suitable direction that aligns with the agent’s specific intentions. The detailed methodology and prompt are detailed in Appendix D.2.

\*\*<https://www.selenium.dev/>

### C.3. Mapping

The mapping module in our environment is designed to equip agents with functionalities such as route planning and transportation time estimation. It mainly utilizes the “Directions API”<sup>††</sup> from the Google Map Platform to facilitate these capabilities. Given the complex nature of this API’s interface, our principal focus has been on parsing its output and adapting it into various user-friendly interfaces for agents.

### C.4. Place Info & Search

Place Info & Search module hosts another important information source in our platform beyond the visual street view imagery, enabling agents to interact with real-world “places”. It provides various attributes of places, including type, name, location, imagery, reviews, etc. In this module, our technical efforts are primarily focused on understanding, comparing, and integrating the most suitable functions from the vast array of Google Maps Platform APIs related to place information and nearby place searches. Additionally, we devise some post-processing strategies to identify and eliminate invalid or conflicting data sources from the Google Maps Platform.

Another essential capability enabled by this module is to associate object proposals in street view imagery and their corresponding places in the real city. This function is vital to enhance the reality of our platform by connecting street view and geolocation. It also powers the “Hiro” agent and the evaluation of the *V-IRL Place* detection benchmark. The implementation is detailed in Sec. 5.2.

## D. Low-Level System Case Study: Intentional Explorer “Hiro”

This section delves deeper into the low-level implementation details of the Intentional Explorer agent “Hiro” (Sec. 3.3), focusing on the prompts utilized to interact with various parts of our system. Concretely, we present the prompts in four subparts: *identifying a type of place to search using the user-defined intention* (Appendix D.1), *selecting appropriate roads* (Appendix D.2), *summarizing reviews of places* (Appendix D.3), and *making action decisions* (Appendix D.4). These four components jointly enable Hiro to explore in our interactive embodied environment driven by his initial intention.

### D.1. Intention to Place Type

Starting with a user-defined agent intention, Hiro first determines the type of place that could fulfill this intention using GPT-4 and the following prompt:

<sup>††</sup><https://developers.google.com/maps/documentation/directions>

```
[Role]
You are PlaceSuggesterGPT, an expert
in recommending types of places
based on user-specified intentions.
```

```
[Task Description]
Given a user-specified intention,
determine the type of "place"
one should seek to fulfill the
intention. Your response should
be in the following JSON format:
{"place": "Desired Place Type"}
```

```
[Example]
Input: "Intention: <buy a book>"
Output: {"place": "bookstore"}
```

```
[Input]
Intention: <{agent_intention}>
```

```
[Output]
Your recommended place type based on
the user-specified intention, in the
required JSON format:
```

Using this prompt with the intention

*Hiro is hungry and looking for a place where he can try some good local food. He cannot handle spicy food.*

returns the result

```
{"place": "restaurant"}.
```

The identified place type (here, `restaurant`) is extracted and set as the target category for Hiro’s open-world detector during his exploration.

### D.2. Road Selection

Whenever Hiro is at a crossroads, he determines the best road to follow using his multi-modal LLM and GPT-4. The primary goal of the road selection process is to identify the road most likely to lead to the desired place type that aligns with Hiro’s intention. First, Hiro fetches the street view towards each potential road using the *V-IRL* environment. Then he utilizes his multi-modal LLM (such as Instruct-BLIP [19] or LLaVA [46]) to generate captions for each road using the following prompt:

```
I am looking for a {place_type}.
Please detail information that might
be helpful for me along this road:
```

Captions for each road are then formatted in the style of

```
{road_idx}: {road_description}
```

and concatenated to form `all_road_descriptions`. These road captions, along with Hiro’s user-defined intention, are then fed into `GPT-4` to determine the most promising road to follow using the following prompt:

```
[Role]
You are PathSelectorGPT, an expert
in choosing the optimal road from
multiple candidates based on a
user-specified intention.
```

```
[Task Description]
Given an intention, the road
previously traveled, and
descriptions of available candidate
roads, select the best road from the
crossroad. Your response must be in
the following JSON format:
{"idx": "Selected road index",
"reason": "Justification for your
selection"}
```

```
[Example]
For the intention "find a grocery
store", the road previously traveled
as "1", and with candidates "2:
Leads to residential area, 3: Leads
to a shopping district", the output
might be: {"idx": "3", "reason":
"Road 3 leads to a shopping district
which is more likely to have a
grocery store."}
```

```
[Input]
User Intention: <{agent_intention}>
Road Descriptions:
{all_road_descriptions}
Previously Traveled Road: Road
{from_road_idx}

[Output]
Your chosen road index and the
reasoning behind your selection,
in the required JSON format:
```

We design such a two-stage captioning and decision-making pipeline for road selection because Multi-modal LLMs cannot process multiple images simultaneously. However, with the recent advancements of GPT-4V, it may be possible to perform road selection using several road images with a single prompt at once. Empirical findings suggest that GPT-4V yields more reasonable choices with the following prompt:

```
[Role]
You are PathSelectorGPT, an expert
in choosing the optimal road from
multiple road images according to a
user-specified intention.
```

```
[Task Description]
Given a set of road images, select
the best road from the crossroad.
Your answer must be in the following
JSON format:
{"idx": "Selected road index (start
by 0)", "reason": "Justification
for your selection"}
```

```
[Input]
User Intention: <{agent_intention}>
```

```
[Output]
Please answer with the road index
and the reasoning behind your
selection, in the required JSON
format:
```

An example road selection response for the first crossroad selection in Fig. 6 is as follows:

★ “idx”: “0”, “reason”: “Choosing road 0 promises a genuine taste of local cuisine in a less commercialized setting. It’s likely to have family-run eateries where I can request non-spicy dishes and savor authentic flavors. This road offers a tranquil dining atmosphere, allowing for a more engaged and leisurely culinary exploration among the locals.”

### D.3. Summarize Place Reviews

When Hiro discovers a place in the street view imagery, he retrieves its corresponding name and Google reviews from the V-IRL environment. There is a complex algorithm behind projecting the 2D box on street view imagery to a concrete place in the real world, which is detailed in “matching between object proposal and places” of Sec. 5.2. After Hiro obtains these place reviews, he summarizes them into a place overview (to aid in decision-making) using the following prompt:

```
[Role]
You are SummarizeGPT, skilled at
condensing multiple reviews into a
concise overview of a location.
```

```
[Task Description]
Given multiple reviews with ratings,
craft a brief overview of the place.
Your response should be in the
following JSON format:
{"summarization": "Concise
description (limited to 80 words)"}
```

```
[Example]
For reviews "Great ambiance but
average food (Rating: 3)" and
"Loved the decor, food could be
```

better (Rating: 3.5)", the output might be:

```
{
  "summarization": "The place boasts great ambiance and decor, but the food quality receives mixed reviews."
}
```

[Input]  
Reviews: **{all\_reviews}**

[Output]  
Your concise overview (max 80 words) based on the provided reviews, in the prescribed JSON format:

#### D.4. Action Decision

After obtaining the overview of the identified place, Hiro decides to visit the place or keep exploration using GPT-4 and the following prompt:

[Role]  
You are ActionSelectorGPT, proficient in choosing the most appropriate action based on a user's background, intention, and an overview of a place.

[Task Description]  
Evaluate the provided user background, intention, and place overview to select the most suitable action from the list. Your response should be in the following JSON format:

```
{
  "action": "Selected Action",
  "reason": "Justification for your choice"
}
```

Possible actions:  
- enter\_place(): Enter the designated place.  
- continue(): Continue searching for another appropriate place.

[Example]  
For the background "loves historical sites", intention "discover local history", and place overview "This is a 200-year-old preserved mansion", the output might be:

```
"action": "enter_place()",
"reason": "The historical mansion aligns with the user's interest in historical sites."
```

[Input]  
User Background: **<{background}>**

User Intention: **<{intention}>**  
Place Overview: **<{place\_intro}>**

[Output]  
Your chosen action and the rationale behind your decision in the prescribed JSON format:

Hiro's exploration will continue if he decides to continue() and will terminate if he opts for enter\_place().

## E. V-IRL Benchmarks: Details

### E.1. V-IRL Places: Detection (Details)

**All category results.** Due to the page limit of the main paper, we only present the results of 10 categories in Tab. 3. Here, we present the place recall for all 20 categories in Fig. 18.

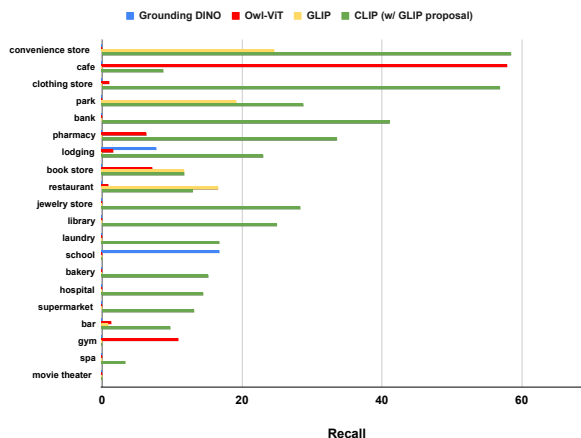


Figure 18. Recalls in V-IRL Place detection

**Example illustrations.** To facilitate the understanding of V-IRL Place detection benchmark, we present some examples of CLIP (w/ GLIP proposals) in Fig. 22.

**Error Diagnosis of Detectors.** We conduct error diagnosis for detectors in the V-IRL Place detection benchmark. We examine two error types: localization error and classification error. As depicted in Fig. 19, the primary challenge arises in classification, where detectors struggle to assign correct labels, despite having accurate object proposals.

### E.2. V-IRL Places: Recognition and VQA (Details)

**Place types performance for recognition.** In Figure 20, we present the averaged accuracy for each place type across 10 benchmarked vision models. The size and the x-axis position of each bubble correspond to the number of places within each type. A clear trend emerges: accuracy tends

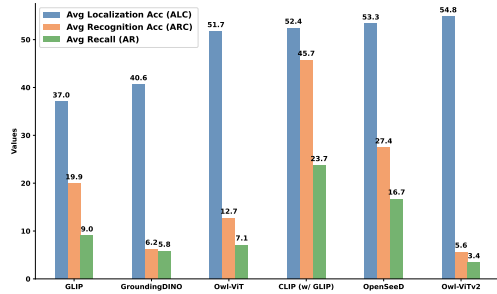


Figure 19. Error diagnosis in *V-IRL Place* Detection

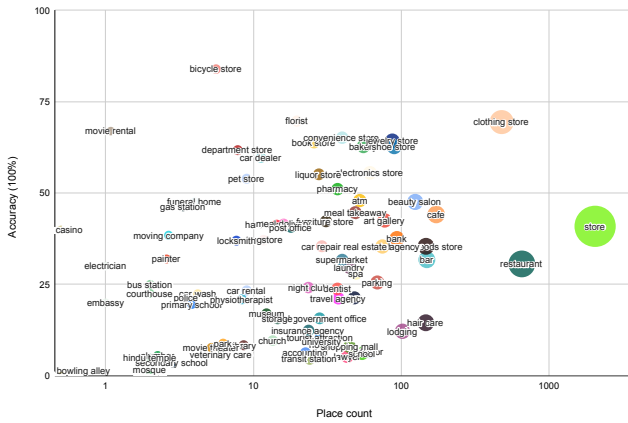


Figure 20. Category-wise accuracy and numbers for *V-IRL Place* Recognition benchmark.

to correlate with the frequency. Common categories such as clothing store, cafe exhibit higher accuracy, whereas vision models often struggle with infrequent place types like bowling alley or mosque.

**Place types performance for VQA.** The place types performance of the *V-IRL* place VQA in Fig. 21 further verifies the correlation between accuracy and frequency from a human intention perspective. The top-10 categories are closely aligned with the most common human activities, purchasing and dining. In contrast, the bottom-10 place types relate to places that are less frequently encountered and serve a more diverse purpose, such as mosque, plumber and embassy.

**Consistency Analysis of *V-IRL Place* VQA Results.** Here, we study the *sensitivity of MLLM to the order of QA options* in VQA. As shown in Tab. 7, advanced MLLMs still exhibit 4.5%-10.6% mAcc drop with circular evaluation. This highlights that MLLMs are still sensitive to the order of QA options presented.

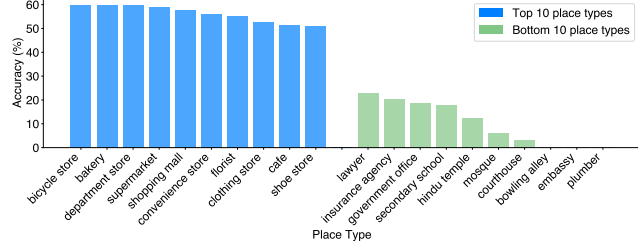


Figure 21. Top-10 and bottom-10 place types averaged on four vision models of *V-IRL Place* VQA.

Method	InternVL-1.5 [17]	GPT-4V [2]	Qwen-VL-Max [9]
mAcc (w/ circular)	77.6	77.1	74.3
mAcc (w/o circular)	82.1	83.1	84.9
<b>mAcc drop</b>	<b>-4.5</b>	<b>-6.0</b>	<b>-10.6</b>

Table 7. MLLM consistency analysis on *V-IRL Place* VQA benchmark.

### E.3. *V-IRL* Vision-Language Navigation (Details)

**Navigation pipeline.** As mentioned in Appendix B.7, our VLN pipeline is similar to [65], however, our benchmark offers greater scalability through the worldwide *V-IRL* platform and an automated data collection pipeline, as opposed to the manual annotation of a specific region. Furthermore, our benchmark emphasizes the analysis of the *vision* component in the VLN pipeline, as opposed to [65], which aims to enhance performance on existing VLN datasets using LLMs.

**Implementation Details.** Here, we introduce the implementation details for LLaVA-1.5 [45] and PP-OCR [23] (+ GPT-3.5). For LLaVA-1.5 [45], we transform the landmark recognition task to a *multiple choice VQA* problem, asking

Which of the following landmarks can be identified with a high degree of confidence?

The VQA options include all potential landmarks mentioned in the route description, along with a “None of above” choice. The model’s response to this question is then parsed as the landmark observation.

For PP-OCR [23] (+ GPT-3.5), we first extract all recognized text using PP-OCR [23] for each street view image. Then, GPT-3.5 [63] determines the presence of each landmark in this street view image, jointly considering the OCR text and landmark name.

**Full set results.** Apart from the mini-set results presented in Sec. 5.4, we also provide the full set results of Oracle and CLIP (L/14@336px) in Tab. 8. The Oracle results, interestingly, do not achieve a 100% success rate, due to incorrect decisions made by the LLM at stop positions. This is evidenced by the high arrival ratio and low reaction accuracy



at stop positions. Empirically, we observe that the LLM occasionally decides to keep moving, despite clear destination indications in the observations.

When we substitute the map in oracle with the CLIP model to gather landmark observations from street view imagery, we observe a significant drop in the success rate, due to the inevitable model prediction errors. To improve the success rate in VLN, we can focus on two important factors: (i) designing better vision models; (ii) developing LLMs and prompt techniques that are robust to vision-related noise. Especially, our empirical findings suggest that sophisticated prompt designs significantly improve the robustness of LLMs to visual observation noise.

Method	Success	Start Intersection			Stop	
		Reac	Arr	Reac	Arr	Reac
Oracle (No Vision)	0.88	1.0	0.95	0.99	0.96	0.88
CLIP (L/14@336px)	0.22	0.84	0.66	0.90	0.61	0.22

Table 8. Results of V-IRL VLN-full.

